Appendix B

Update of the Idaho Waste Area Group 3, Operable Unit 3-13 Group 5 Groundwater Numerical Model

Appendix B

Update of the Idaho Waste Area Group 3, Operable Unit 3-13 Group 5 Groundwater Numerical Model

B-1. INTRODUCTON

Modeling the Snake River Plain Aquifer (SPRA) for the *Comprehensive RI/FSfor the Idaho Chemical Processing Plant OU 3-13 at the INEEL—Part A, RI/BRA Report (Final)* (DOE-ID 1997) predicted a risk beyond the year 2095 to groundwater users. High concentrations of 1-129 were predicted to remain in the low-hydraulic conductivity HI sedimentary interbed. However, the OU 3-13 remedial investigation/baseline risk assessment (RI/BRA) modeling was performed using only a limited amount of empirical data for parameterizing the HI interbed, and no empirical data were available for verifying the presence or absence of contaminants in the interbed.

The OU 3-13 RI/BRA aquifer model was updated during OU 3-13, Group 5 remedial actions (DOE-ID 2000). The modeling update was performed to assess model sensitivity to key parameters and identify data needs as well as to support field activities to collect empirical data. The aquifer model update included rediscretization and reparameterization to more accurately simulate the HI interbed and deep aquifer. Recent aquifer characterization work by Smith (2002) has shown deep well temperature logs can be used to estimate active aquifer thickness. The relatively isothermal temperature gradient in the temperature logs suggest water is moving fast enough to overcome the geothermal gradient and identify the actively flowing portion of the aquifer. The updated flow model was calibrated to more recent aquifer potentiometric measurements and the transport model was calibrated to the tritium disposal in the CPP-03 well.

Field and laboratory testing performed for this report provided vertical profiling of 1-129, Sr-90, Tc-99, tritium concentrations, and geotechnical data across the HI interbed at three borings downgradient of the Idaho Nuclear Technology and Engineering Center (INTEC). These data were used to adjust the current model's interbed parameterization and contaminant source terms to be consistent with the latest observations. Furthermore, the 1-129 source term was revised by analysis of historical INTEC processes. The results are documented in this report. Section B-2 presents the current WAG 3 aquifer numerical model, Section B-3 presents the current model's predictive simulations of the Group 5 focus contaminants (tritium, Tc-99, Sr-90, and I-129), and Section B-4 presents the modeling conclusions.

B-2. CURRENT WASTE AREA GROUP 3 AQUIFER MODEL

This section of the appendix describes the revised SWA groundwater flow and transport model and results.

B-2.1 Model Purpose

The remediation goals of OU 3-13, Group 5 are to monitor groundwater concentrations and perform treatability studies if groundwater concentrations exceed the specified action level. The numerical model will be used to assess the effectiveness of different remedial scenarios, assess future concentrations from current observations, or adjust the action level.

Updating the Group 5 aquifer model will coincide with updating the Group 4 aquifer model and developing the OU 3-14 aquifer model. The contaminated perched water addressed by the Group 4 remediation goals does not pose a risk to human health, because it is not available for consumption. However, the perched water does pose a risk as a contaminant transport pathway to the SWA. The Group 4 aquifer model, along with an updated vadose model, will be used to assess the effectiveness restricting various surface water recharge sources to minimize transport of contaminated perched water to the aquifer.

The purpose of the OU 3-14 aquifer model will be to calculate future risks from contaminants of concern (COCs) identified in the OU 3-14 remedial investigation/feasibility study (RI/FS) and evaluation of proposed remedial actions. The following summarizes the primary anticipated uses of the OU 3-14 simulation results:

1. Baseline Tank Farm risk evaluation from the groundwater pathway. Aquifer concentrations will be predicted and used for the risk assessment.

2. Baseline cumulative risk evaluation. The cumulative risk from all the INTEC sources, including OU 3-14 sources, OU 3-13 sources excluding Tank Farm source, and INEEL CERCLA Disposal Facility (ICDF) sources.

3. Evaluation of proposed remedial actions. During the feasibility study phase of the OU 3-14 RI/FS, remedial action alternatives will be recommended and the model will be used to evaluate the effectiveness of these alternatives.

B-2.2 Model Description

The physical and hydrogeologic setting of INTEC is highly complex, consisting of alternating layers of basalt and sediments. In the vadose zone, numerous perched water bodies have formed beneath surface recharge sources. The aquifer's geology is more uniform in the vertical direction than that of the vadose zone. The aquifer basalt units tend to be thicker than the vadose zone basalt flows, and the sedimentary interbeds are fewer in number. United States Geological Survey (USGS) studies (Anderson and Lewis 1991) indicate that the aquifer in the region north of INTEC and extending south of the Radioactive Waste Management Complex (RWMC) is comprised primarily of the E through H basalt flows, the HI interbed, and the I basalt flow. The I basalt flow is significantly thicker (Anderson and Lewis 1991). The I basalt flow may have a lower permeability than the E through H basalt flows, because the high permeability interflow rubble zones represent a smaller fraction of the total flow thickness. The HI sedimentary interbed separates the two basalt flows.

The WAG 3 aquifer modeling was performed using the TETRAD multipurpose simulator software (Vinsome and Shook 1993). The aquifer model domain extends from approximately 2.5 km north of the INTEC facility to the southern Idaho National Engineering and Environmental Laboratory (INEEL) boundary in the north-south direction, and approximately 6.5 km east of the INTEC facility to approximately 1 km west of the RWMC facility in the east-west direction. The model was discretized into 400 x 400 grid blocks in the horizontal, as illustrated in Figure B-1. Local horizontal refinement corresponding to the discretization level applied in the OU 3-13 RI/BRA vadose zone model is used for the INTEC footprint (200 m x 200-m grid block size) and also in the vicinity of Test Reactor Area (TRA). This local refinement was only performed in the aquifer model's top layer. The model used variable vertical discretization that followed the HI interbed. as discussed in Section B-2.2.

The aquifer model used four distinct stratigraphic types. These include the E through H basalts, the upper I basalt, the HI interbed, and the lower I basalt. The upper I basalt was defined as the top 25 m of the aquifer where the I basalt flow is at or above the water table. This part of the I basalt flow was separated from the majority of the I basalt flow, because it is at the water table and wells are completed in this area of the I basalt flow, providing a pump-test-based permeability field. The initial permeability values for the current model's H basalt and upper I basalt were created from a spatial correlation analysis of pumping test permeability values in INEEL wells. Initial permeability values for the current model's HI interbed were estimated from pumping test and core analysis of the HI interbed. Initial permeability values for the current model's I basalt were taken from the early WAG 10 modeling effort (McCarthy et al. 1995). Initial estimates of model transport parameters (porosity and dispersivity) also were taken from the RI/BRA aquifer model. Figure B-2 illustrates the initial H basalt hydraulic conductivity field and includes the pumping test data.

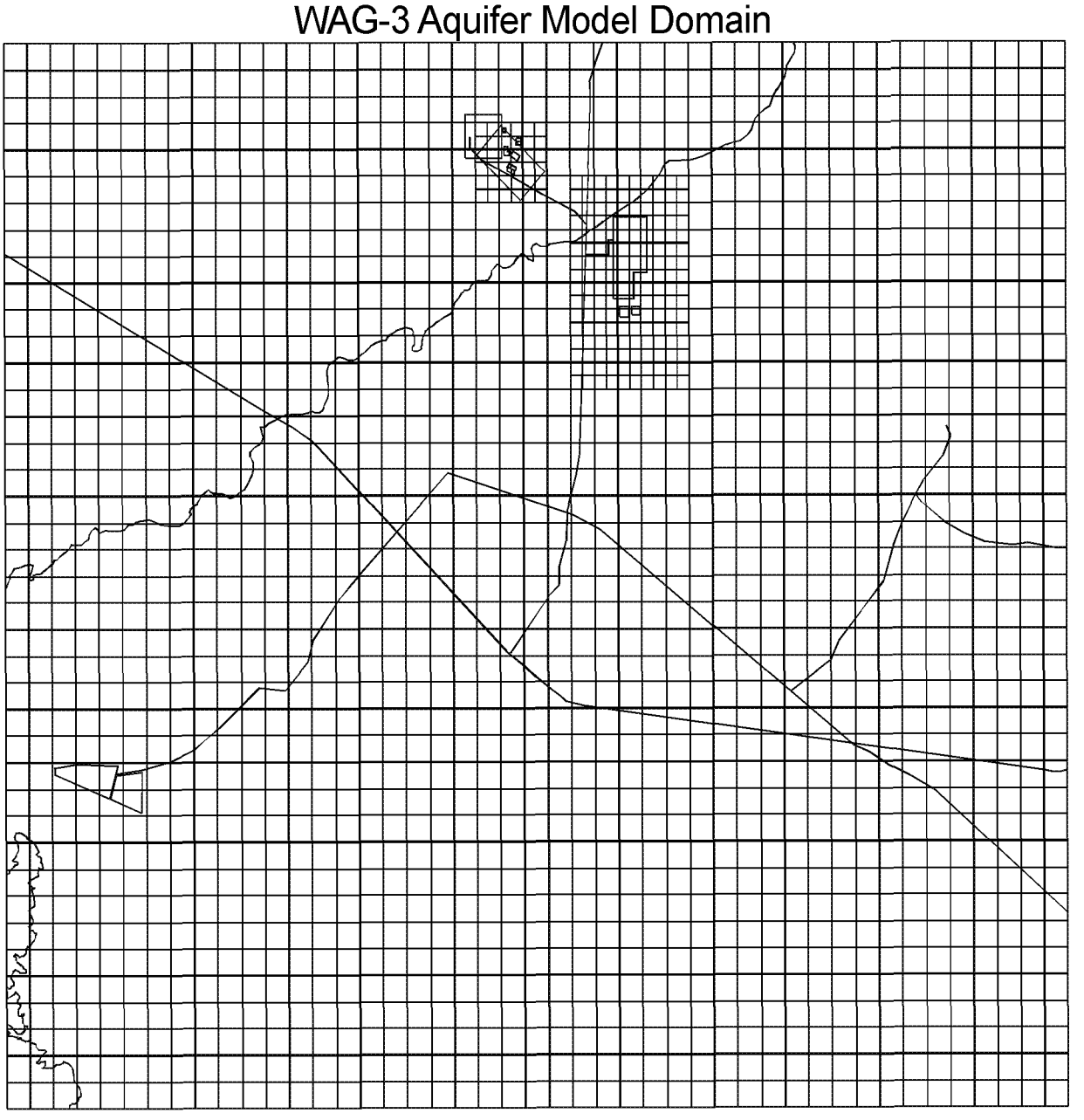

Figure B-1. Aquifer model domain and horizontal discretization.

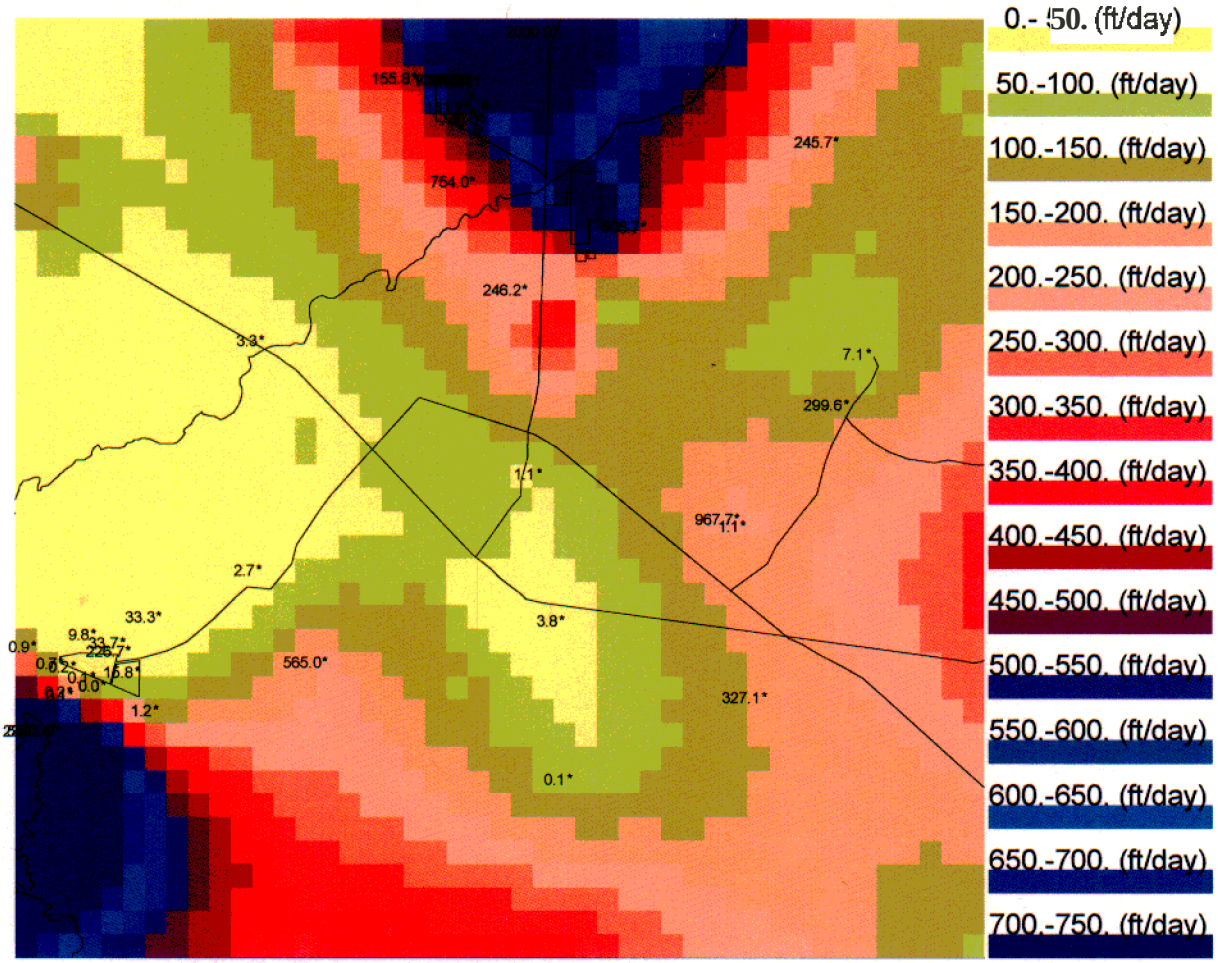

Figure B-2. Initial H basalt hydraulic conductivity estimate.

There is only a limited amount of information available on the permeability of the HI interbed. Pumping tests have been performed by the State of Idaho (Frederick and Johnson 19%) using packers to isolate the interbed from the surrounding basalt. Geotechnical analysis of interbed samples collected for the present investigation from Boreholes ICPP-1795, ICPP-1797, and ICPP-1798 (hereafter referred to as the vertical profile boreholes) also has provided permeability estimates south of INTEC. The results of the pumping tests and geotechnical analysis are provided m Table B-1. Both the basalt and interbed parameters were adjusted during the current model's calibration, which is discussed in Section B-2.4.

The Big Lost River flows across the aquifer model domain and the long-term average infiltration from the Big Lost River was applied directly in the aquifer model outside the area of the RI/BRA vadose zone model footprint (see refined area around INTEC in Figure B-1). Infiltration within the footprint was accounted for indirectly through the water and contaminant flux boundary condition from the vadose zone model. In addition to the Big Lost River, the pumping from the water supply wells (CPP-02, CPP-04, CFA-1, and CFA-2) and reinjection into the former injection well (CPP-03) were included in the simulations. The boundary conditions for the aquifer model were specified flux at the surface (including the water sources discussed above), no flux at the bottom, and specified heads on the sides.

Table B-1. Summary of HI interbed permeability values.

Well	Hydraulic Conductivity (ft/day)	Permeability (mD)	Reference
USGS-44	0.273	9.99E+01	Fredrick and Johnson 1996, Table 11
USGS-45	0.216	7.89E+01	Fredrick and Johnson 1996, Table 11
USGS-46	0.216	7.89E+01	Fredrick and Johnson 1996, Table 11
USGS-59	0.101	3.68E+01	Fredrick and Johnson 1996, Table 11
ICPP-1795	2.78E-04	0.101	DOE-ID 2003, Table 3-4
ICPP-1795	6.52E-04	0.238	DOE-ID 2003, Table 3-4
ICPP-1797	34.0	1.24E+04	DOE-ID 2003, Table 3-4
ICPP-1797	2.35	859.0	DOE-ID 2003, Table 3-4
ICPP-1798	0.184	67.3	DOE-ID 2003, Table 3-4
ICPP-1798	3.97	1.45E+03	DOE-ID 2003, Table 3-4
Arithmetic mean	4.13	1.51E+03	—
Geometric mean	0.163	59.70	—

ICPP = Idaho Chemical Processing Plant
USGS = United States Geological Survey

B-2.3 Current Aquifer Model Vertical Discretization

The OU 3-13 RI/BRA aquifer model has been rediscretized from that used in the RI/BRA modeling to more accurately simulate the HI interbed, because the OU 3-13 RI/BRA simulations indicated the HI interbed was primarily responsible for maintaining elevated I-129 concentrations. The current model's bottom surface was created from active aquifer thickness estimates provided by Smith (2002). Smith used deep well temperature logs to estimate thickness of the active aquifer. The relatively isothermal temperature gradient in the upper part of the temperature logs are attributed to cold recharge water moving fast enough to overcome the geothermal gradient and identifying the actively flowing portion of the aquifer. The number of deep wells, which fully penetrate the entire aquifer, is very limited and a large amount of interpolation was needed to create the model's bottom surface. Figure B-3 illustrates deep well locations and the active aquifer thickness at each well. The current model's bottom surface is below the HI interbed at all locations within the simulation domain. Figure B-4 illustrates the simulated aquifer thickness in the current model. The surface illustrated in Figure B-4 is one of many possible realizations of the active aquifer depth in the vicinity of INTEC.

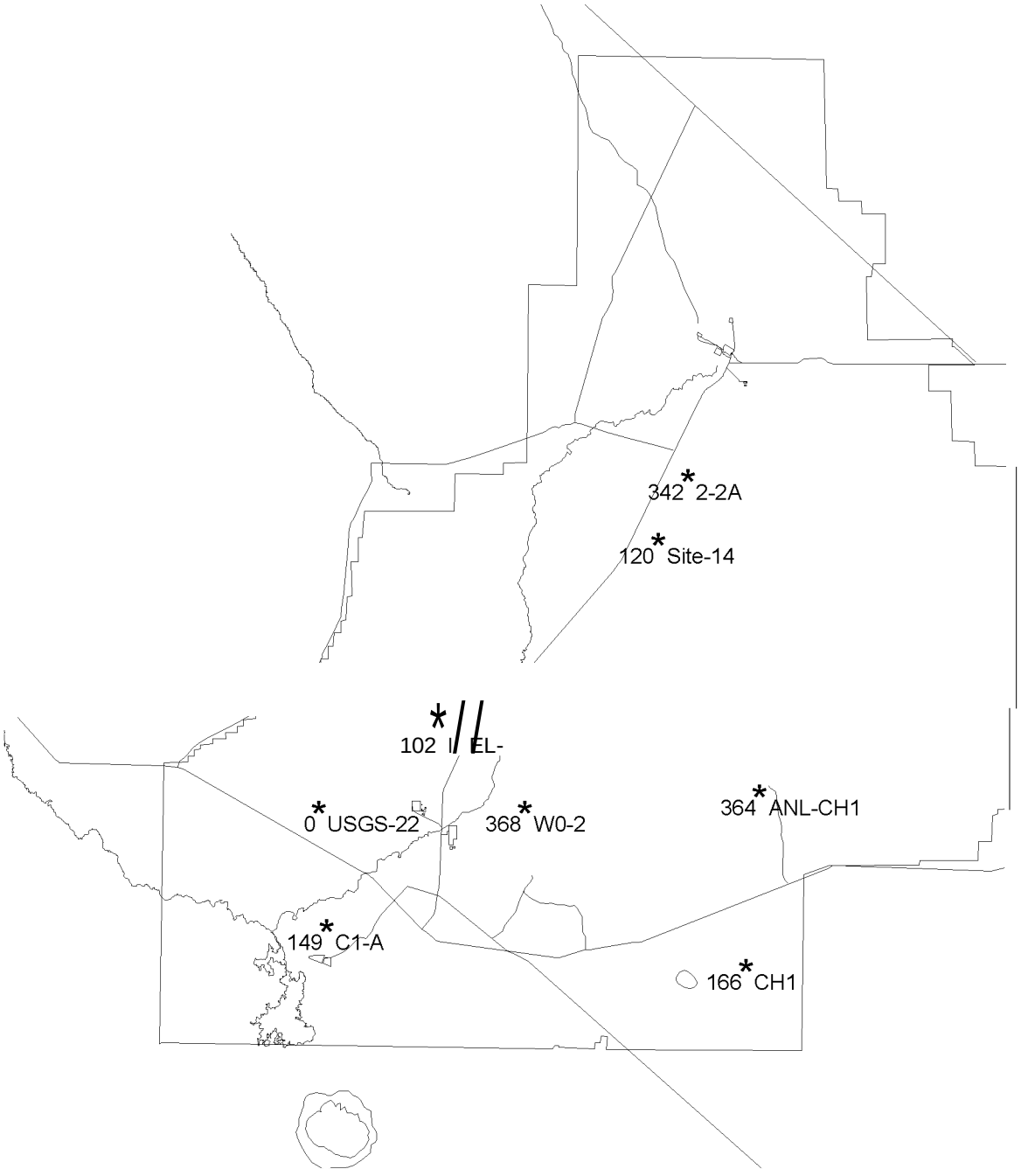

Figure B-3. The INEEL deep well locations and active aquifer depth (m)

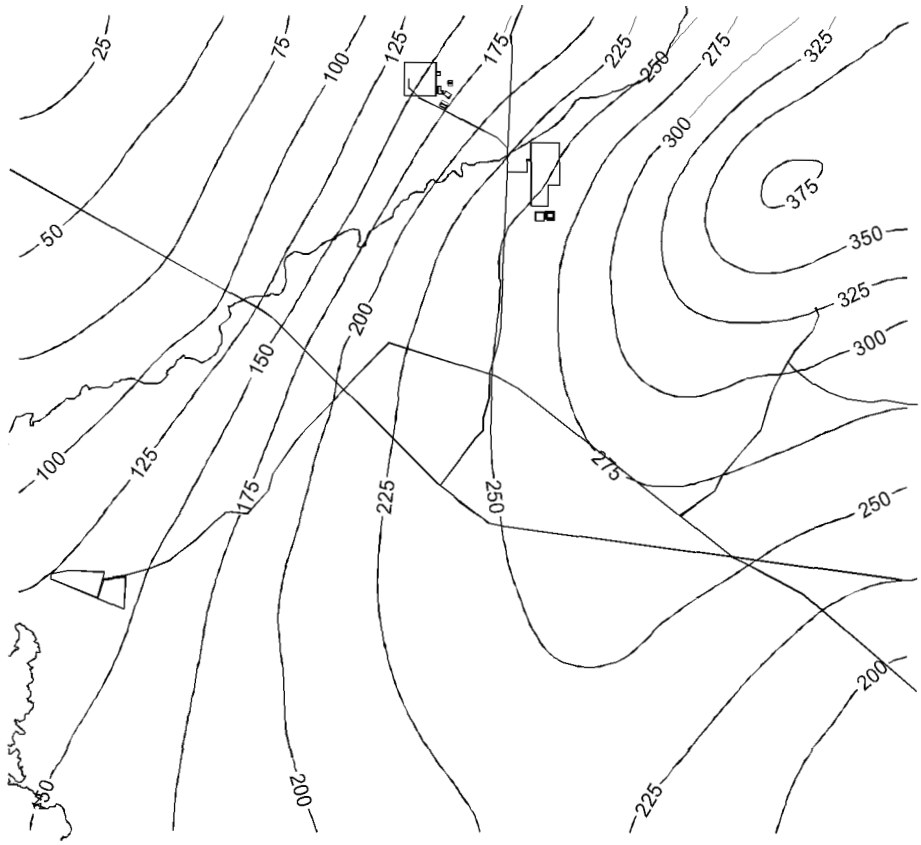

Figure B-4. Current aquifer model thickness (m).

B-2.4 HI Interbed Placement

The HI interbed elevation and thickness data were reviewed and incorporated into the current aquifer model.

B-2.4.1 HI Interbed Depth and Thickness

The HI interbed is a widespread layer of sediment overlying Basalt Flow Group I. The interbed tends to dip in the southeast direction when viewed from a large scale (OU 3-13 RI/BRA aquifer model domain) and the interbed tends to become thicker and more continuous in the southeast direction. Well logs from Wells SPERT-IV and Site-09 (southeast of INTEC) indicate the interbed can be approximately 90 ft thick in some areas.

Data taken from INEEL and USGS well logs for 51 wells were used to define the HI interbed thickness and surface elevation. The HI interbed data pertaining to older INEEL and USGS wells can be found in *Stratigraphy of the Unsaturated Zone at the Radioactive Waste Management Complex, Idaho National Engineering Laboratory, Idaho* (DOE-ID 1989) and *Stratigraphy of the Unsaturated Zone and Uppermost Part of the Snake River Plain Aquifer at the Idaho Chemical Processing Plant and Test Reactor Area, Idaho National Engineering Laboratory, Idaho* (DOE-ID 1991). Some of the data taken from more recent INEEL wells might not have not been published in formal reports. Planes were fitted through both surface elevation and thickness data sets using linear regression. De-trended data sets of the surface and thickness were created by subtracting the fitted planes. Variogram models describing spatial correlation were then fitted to the de-trended data and simple Kriging was used to interpolate the model's

HI interbed structure. The data used to define the HI interbed are contained in Table B-2. Figures B-5 and B-6 illustrate interbed thickness, and Figures B-7 and B-8 illustrate interbed elevation surfaces. Figures B-7 and B-8 include the data used to create the thickness and elevation surfaces.

The HI interbed surfaces presented in Figures B-5 through B-7 differ from those presented in Figures 3-2 and 3-3, because the HI interbed structure was not updated from that used in the year 2000 Group 5 model update (DOE-ID 2000). The data used to create the HI interbed structure did not include the new borings. Furthermore, different interpolation techniques were used and the surfaces presented in Appendix B are those in the model, which could not strictly reproduce the observed data because grid block spacing was larger than the distance between wells.

Table B-2. HI interbed elevation and thickness data.

Well	Well Surface Elevation (ft)	Depth to HI Interbed Top (ft)	HI Interbed Thickness (ft)
CFA-1	4,928.31	623	48
CPP-3	4,916.047	519	7
CPP-4	4,909.282	523	0
LF2-09	4,932.227	625	14*
LF2-10	4,932.477	620	49
MTR-test	4,917.149	351	0
NPR-test	4,933.146	556	42
OW-1	5,042.0	758	5
ow-2	5,044.0	781	6
RWMC-m04d	5,022.53	728	3
Site-09	4,926.9	724	84
Site-19	4,926.329	462	5
SPERT-IV	4,924.0	837	87
TRA-06a	4,926.0	489	6
TRA-07	4,931.0	495	6*
USGS-020	4,916.355	611	65*
USGS-034	4,929.186	593	4
USGS-038	4,929.633	596	5
USGS-039	4,930.951	568	4
USGS-040	4,916.155	527	2
USGS-041	4,916.906	530	4
USGS-042	4,917.85	547	0
USGS-043	4,916.05	516	4
USGS-044	4,917.927	521	0
USGS-045	4,919.63	541	9

Table B-2. (continued).

Well	Well Surface Elevation (ft)	Depth to HI Interbed Top (ft)	HI Interbed Thickness (ft)
USGS-046	4,916.152	542	6
USGS-047	4,916.309	532	5
USGS-048	4,917.11	549	3
USGS-049	4,912.9	540	2
USGS-051	4,918.74	561	4
USGS-052	4,909.557	526	5
USGS-057	4,922.487	567	5
USGS-058	4,918.373	342	7
USGS-059	4,914.53	554	4
USGS-065	4,925.007	490	8*
USGS-066	4,920.768	365	7
USGS-067	4,913.934	572	18
USGS-076	4,929.698	528	4
USGS-079	4,931.083	487	4
USGS-082	4,908.23	557	9
USGS-083	4,942.69	716	36*
USGS-085	4,939.255	631	6*
USGS-104	4,988.651	688	12*
USGS-106	5,015.29	652	0
USGS-121	4,909.646	517	5
USGS-123	4,920.1	559	4
C-1A	5,029.0	698	5
EOCR	4,943.3	966	34
NPRWO-2	4,930	571	27
S5G-Test	4,850	698	26
WS-INEL-1	4,878.43	670	29

* Well did not fully penetrate interbed.
CFA = Central Facilities Area
CPP = Chemical Processing Plant
MTR = Materials Test Reactor
RWMC = Radioactive Waste Management Complex
SPERT = Special Power Excursion Reactor Test
TRA = Test Reactor Area
USGS = United States Geological Survey

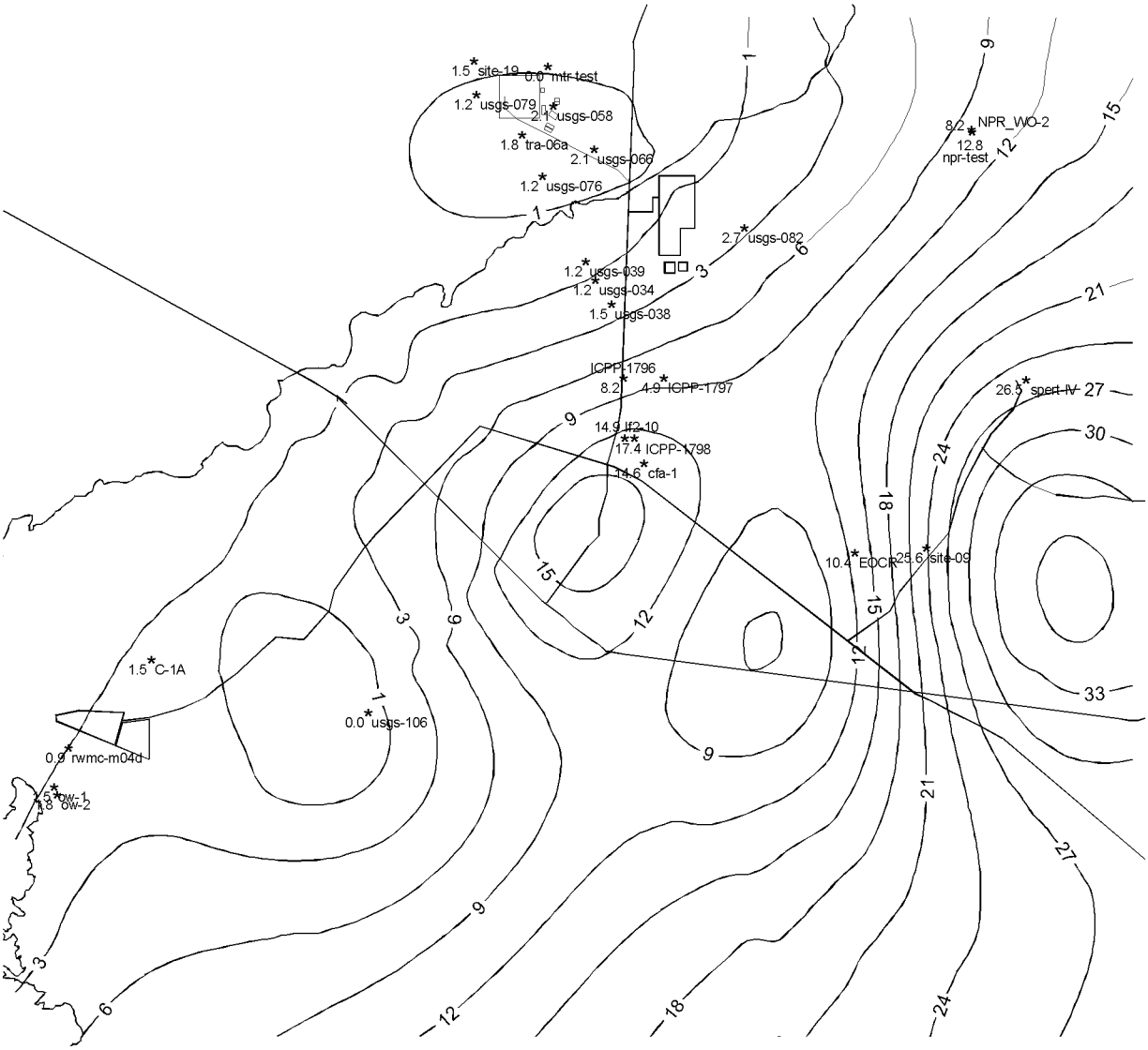

Figure B-5. Current model's HI interbed thickness (m).

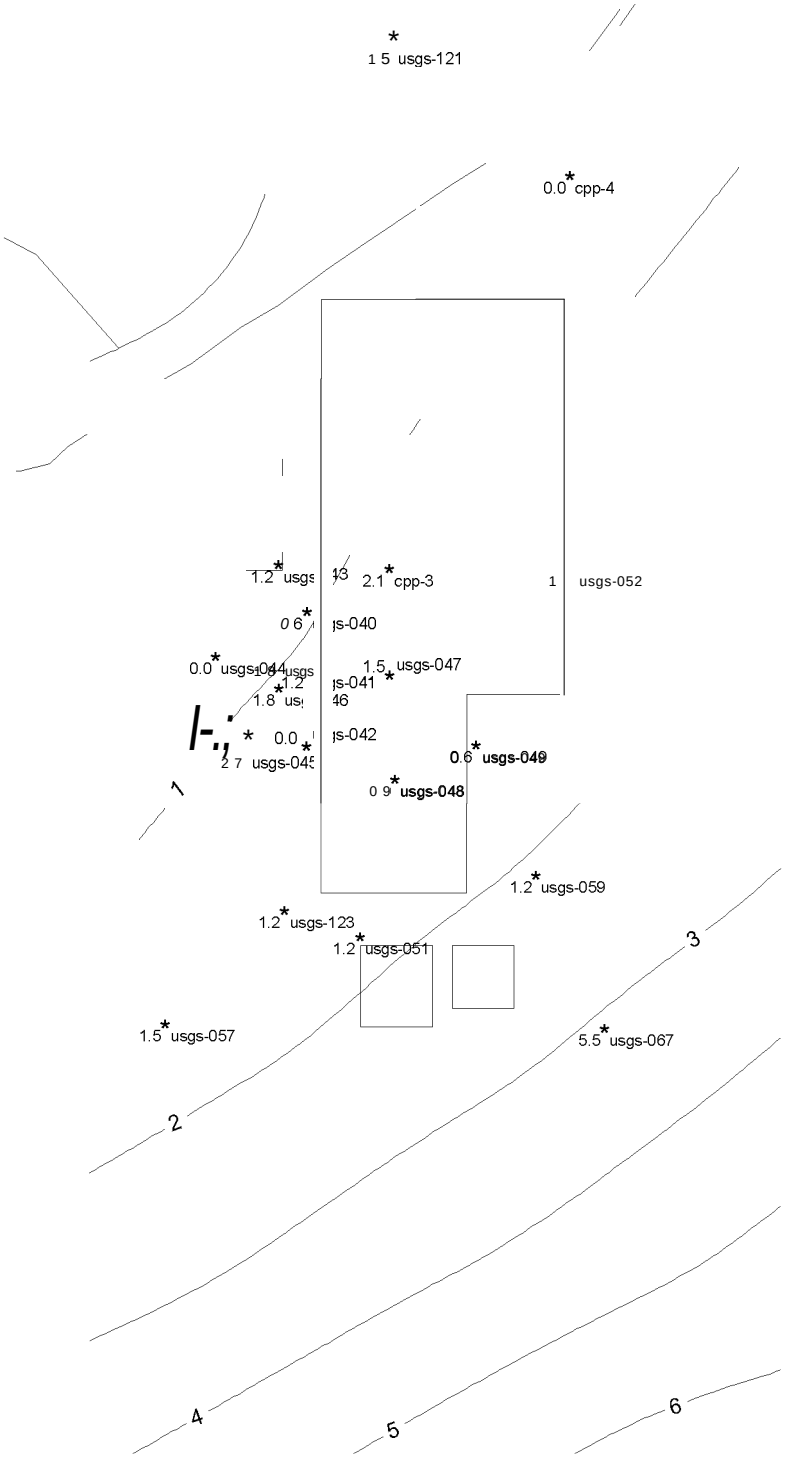

Figure B-6. Current model's HI interbed thickness (m) in the INTEC vicinity.

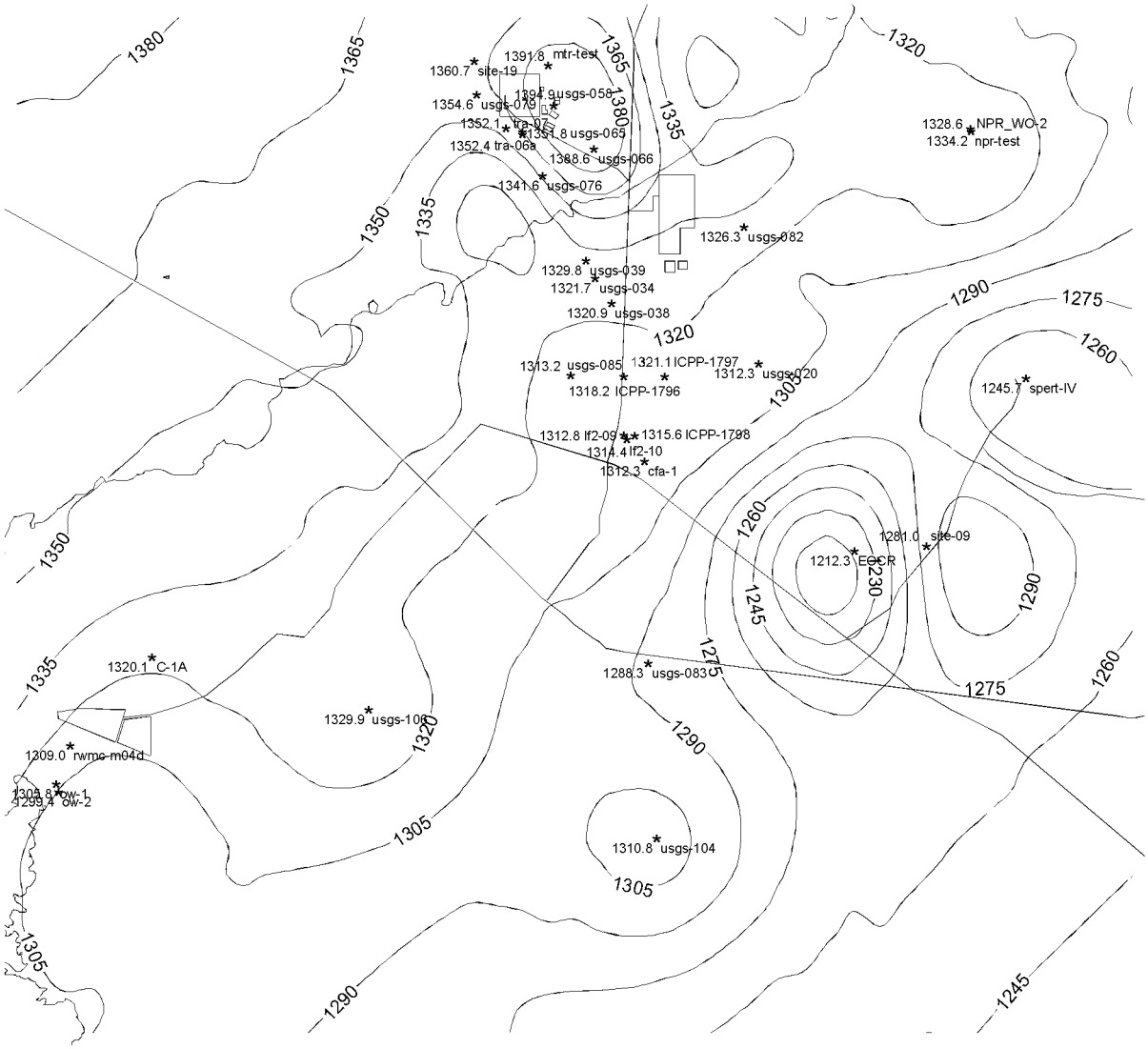

Figure B-7. Current model's HI interbed elevation (m).

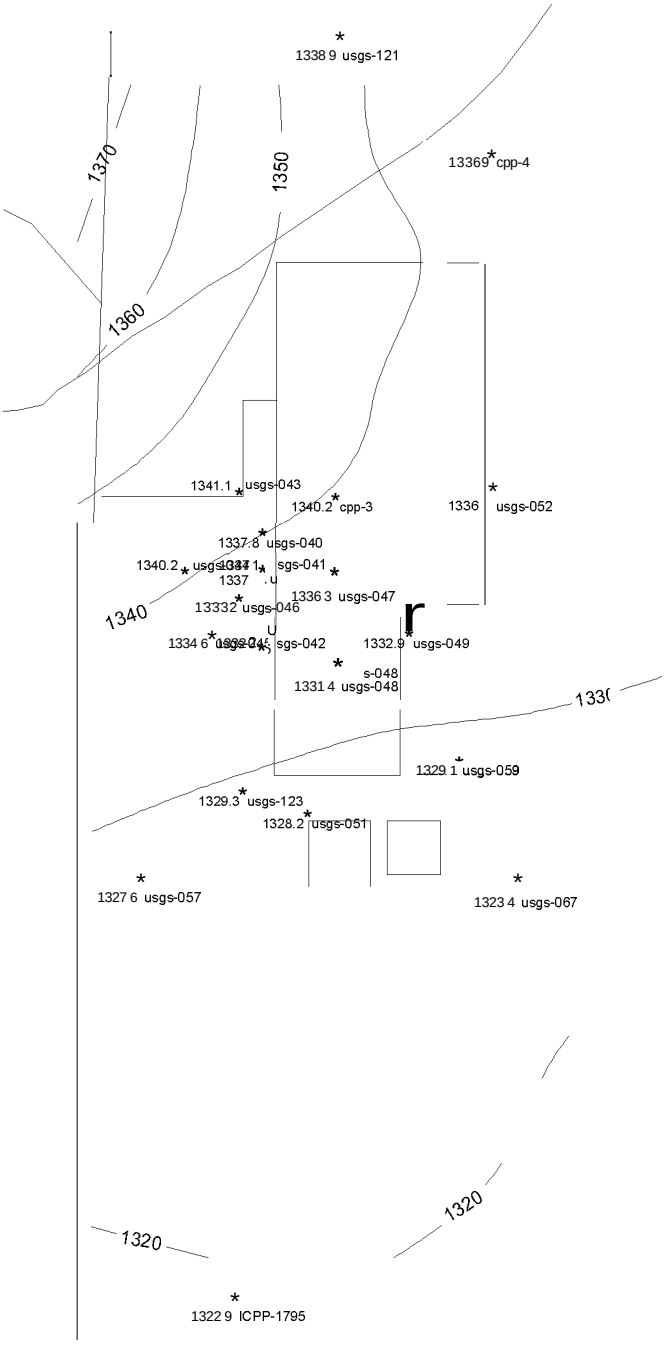

Figure B-8. Current model's HI interbed elevation (m) in the INTEC vicinity.

B-2.4.2 Interbed Rediscretization

The current model's vertical discretization (Figure B-9) followed the HI interbed and placed more computational nodes in and around the HI interbed. Adapting the grid to follow the HI interbed also allowed fewer computational nodes to adequately represent the complex basalt/interbed lithology. The interbed is represented by an average of four model layers, and the minimum thickness is 2 m. The grid block thickness increased with distance above and below the interbed and the current model used 18 layers.

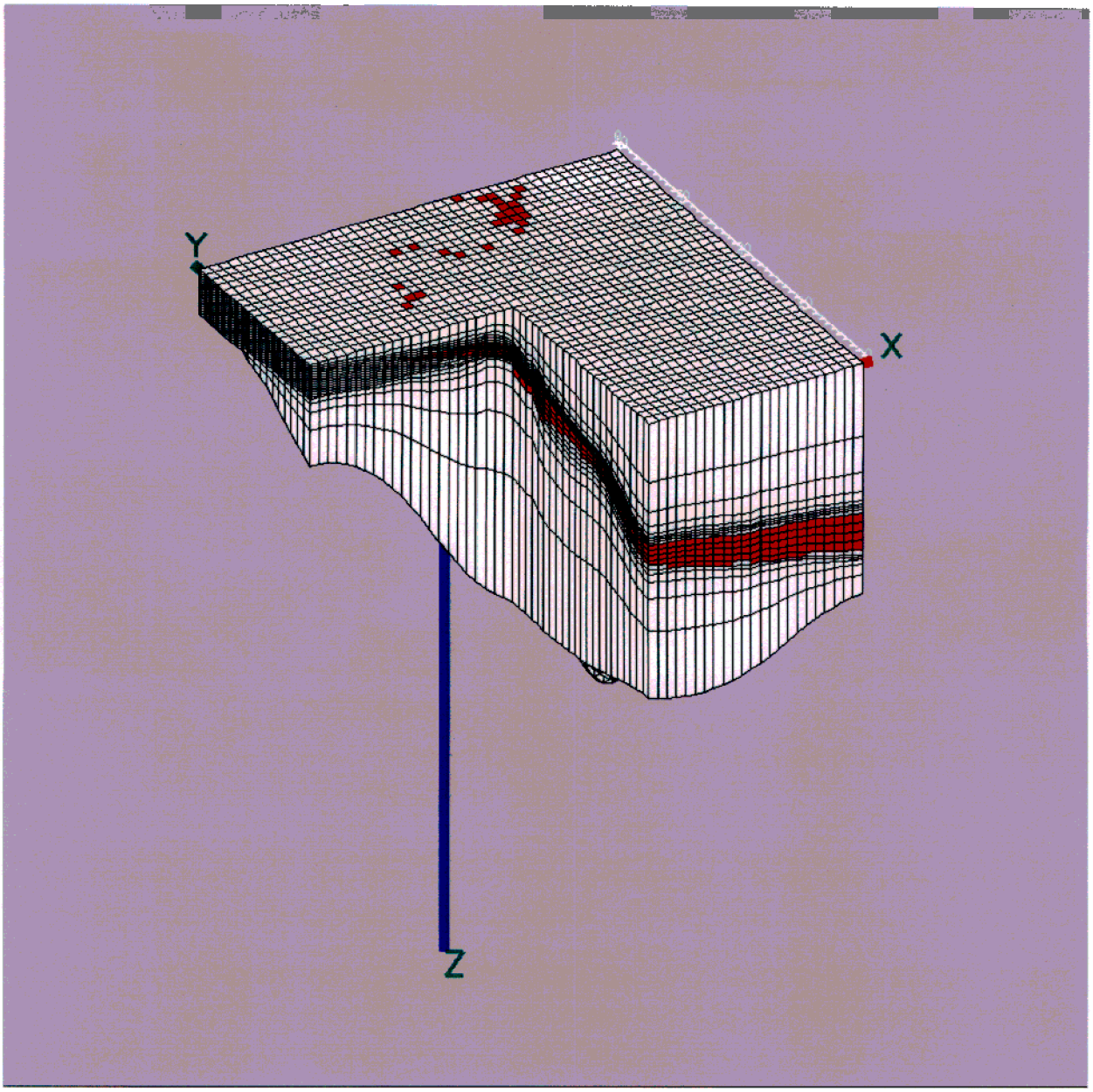

Figure B-9. Current aquifer model vertical discretization with vertical exaggeration.

B-2.5 Current Model Calibration

Calibration of the transport model used the tritium disposal history in the CPP-03 injection well. The tritium disposed in CPP-03 provided *good* calibration data, because the inventory disposed of to the injection well is fairly well defined, and there is a long historical record (1953–present) of tritium activities at USGS Monitoring wells located downgradient.

The match between simulated hydraulic head, tritium concentrations, and the observed values was evaluated with qualitative and quantitative criteria. The qualitative criteria included simulated contour *maps* of the spring 1999 hydraulic head measurements with observed data plotted on the maps and simulated tritium breakthrough curves at USGS observation wells with observed tritium concentrations

overplotted on the curves. The spring 1999 hydraulic head measurements were chosen to evaluate the flow model, because this data set is the most comprehensive measurement for a single time period.

Three statistics were chosen to measure the agreement between field data and simulation results: (1) the root mean square (RMS) error, (2) relative mean absolute deviation (RMAD), and (3) the correlation coefficient. The RMS error was used to evaluate the match between observed and simulated hydraulic head. The RMS error provides a good estimation of the average error throughout the data set and is defined as shown in Equation (B-1).

$$RMS = \sqrt{\frac{\sum_{i=1}^{k}(s_i - f_i)^2}{k}} \qquad \text{(B-1)}$$

where

f_i = field data point

s_i = simulation data point

k = number of comparison points.

The RMAD was used to evaluate the match between observed and simulated tritium concentrations. The RMAD statistic illustrates the average relative error between two data sets. The RMAD is defined as

$$RMAD = \frac{\sum_{i=1}^{k}\left|\frac{s_i - f_i}{f_i}\right|}{k} \qquad \text{(B-2)}$$

If the measured tritium concentration was zero, the concentration was set to 200 pCi/L, which is a typical tritium detection limit, in the divisor (f_i) term of Equation (B-2) to prevent division by zero.

The correlation coefficient was used to evaluate the agreement of the simulated and observed tritium breakthrough curve shape. The correlation coefficient measures the degree to which there is a linear correlation between two data sets. A perfectly linear relationship between data sets would result in a correlation coefficient of 1. Independent data sets would have a correlation coefficient of 0. Data sets, which have a linear relationship but trend in different directions, will have a negative correlation coefficient. The correlation coefficient (r) is defined as shown in Equation (B-3).

$$r = \frac{k\sum_{i=1}^{k} s_i f_i - \sum_{i=1}^{k} s_i \sum_{i=1}^{k} f_i}{\sqrt{\left[k\sum_{i=1}^{k} s_i^2 - \left(\sum_{i=1}^{k} s_i\right)^2\right]\left[k\sum_{i=1}^{k} f_i^2 - \left(\sum_{i=1}^{k} f_i\right)^2\right]}} \qquad \text{(B-3)}$$

B-2.5.1 Aquifer Hydraulic Head Calibration

The best agreement with the spring 1999 hydraulic head data was obtained by slightly adjusting the model's southeast boundary conditions and setting the H basalt minimum permeability to 1,000 mD (2.4 ft/day). A minimum H basalt permeability was needed to prevent extreme mounding from Big Lost River recharge. The current model's hydraulic head RMS error over all wells within the simulation domain was 1.1m. The current model's steady-state flow field with spring 1999 measured hydraulic head is presented in Figures B-10 and B-l 1. It is interesting to note that recharge from the spreading areas located southwest of the RWMC (southwest corner of the simulation domain) may be creating sufficient groundwater mounding to locally reverse the large-scale gradient. The average hydraulic head of four wells immediately west of the spreading area (RWMC-MA65, USGS-120, RWMC-MA66, and RWMC-MA13) is 1,35 1.5 m and average hydraulic head of six wells immediately south of the RWMC (RWMC-M01S, USGS-17, USGS-88, RWMC-M04D, USGS-119, and RWMC-M06S) is 1,350.1m, suggesting water is flowing toward the Subsurface Disposal Area from the spreading area.

B-2.5.2 CPP-3 Injection Well Tritium Disposal Calibration

The best agreement between simulated and observed tritium concentrations was obtained by decreasing basalt porosity to 3%, decreasing the initial basalt permeability estimates by a factor of two, and increasing the dispersivity to 20 m in the longitudinal direction 10 m in the transverse direction.

The vertical sampling performed during 2002 in the ICPP-1795, -1796, -1797, and -1798 wells indicates tritium and 1-129 concentrations are currently higher above and within the HI interbed than below the interbed. The vertical sampling suggests the HI interbed may be acting as a dividing layer between the deep and shallow aquifer, but concentrations are not as different as the earlier modeling indicated. The HI interbed permeability was increased to 500 mD to better match the vertical profiling (DOE-ID 2003).

The current model's porosity was similar to the value needed to simulate the contaminant plume at the Test Area North (TAN). Both the current model and the TAN model departed from previous groundwater modeling of the INEEL by using a variable thickness aquifer based on hydrogeologic data. The QR interbed provided the effective bottom of the contaminated aquifer at TAN and deep well temperature logs provided estimates the actively flowing aquifer below INTEC. Inverse modeling of a large-scale infiltration/tracer test at the INEEL (Magnuson 1995) also showed that an approximately 3% large-scale effective porosity for the fractured basalt matched the observed infiltration data.

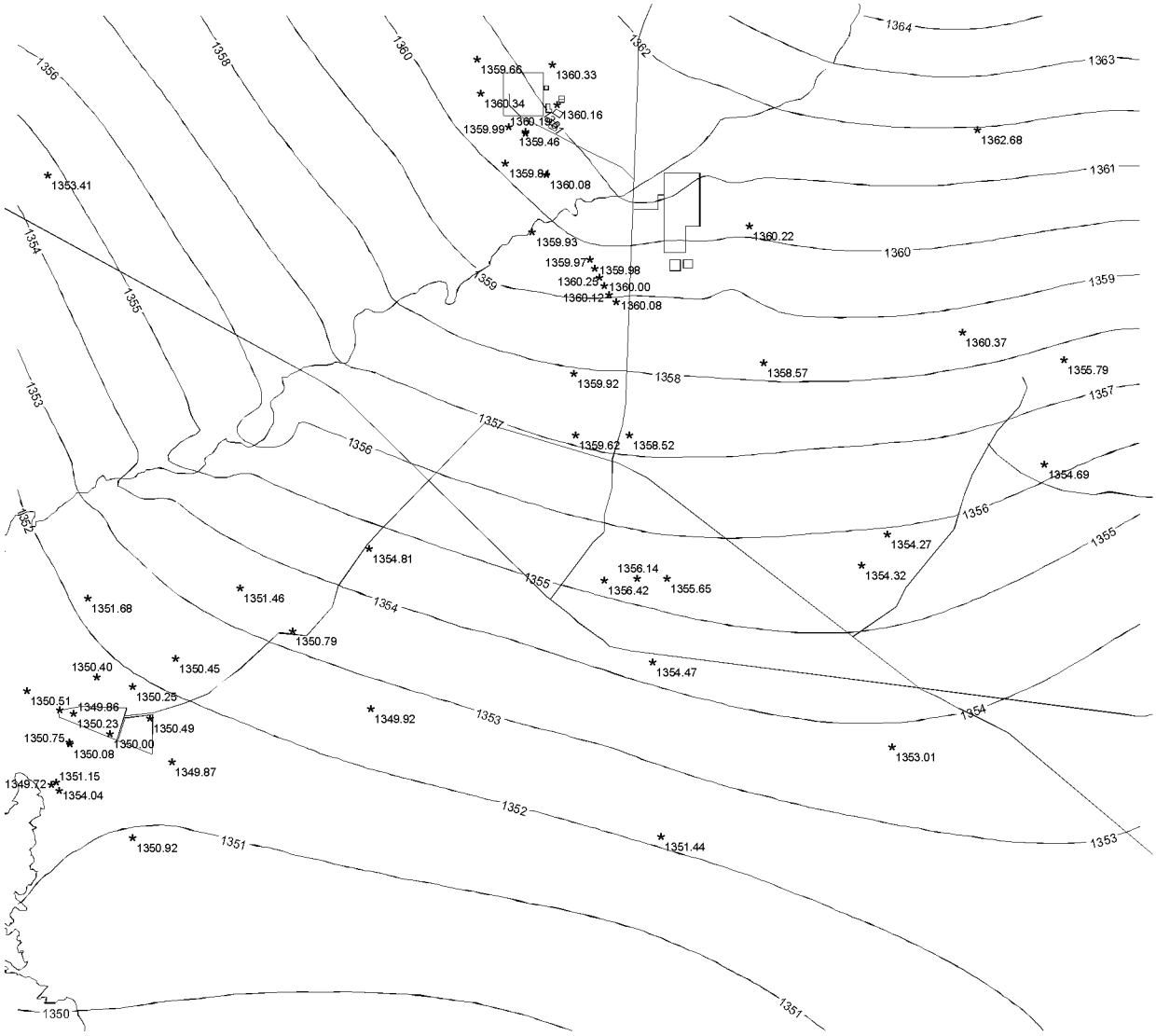

Figure B-10. Current model hydraulic head (m) with spring 1999 observations.

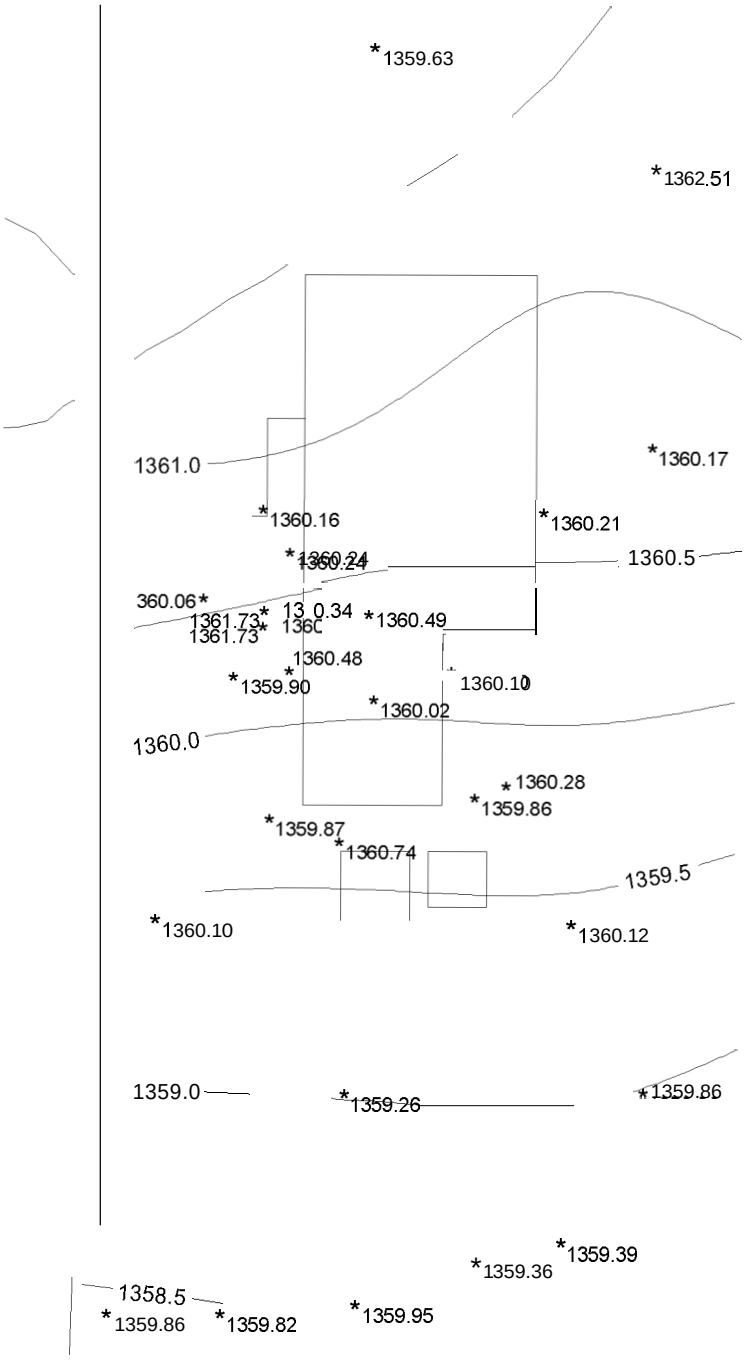

Figure B-11. Current model hydraulic head (m) with spring 1999 observations near INTEC.

Figure B-12 illustrates the CPP-3 injection well tritium disposal history used in the RI/BRA aquifer model calibration. Figures B-13 and B-14 illustrate the locations of the tritium breakthrough calibration wells and Figures B-15 through B-18 illustrates model-predicted breakthrough and observed tritium concentrations for each well. Four data sets are plotted on each well breakthrough plot: (1) observed concentration (thin black line with a cross data symbol), (2) simulated well screen center (thick red line), (3) simulated concentration at the aquifer top (thin dashed green line), and (4) simulated concentration at the aquifer bottom (thin blue line).

Two problems can be seen in the tritium disposal and breakthrough data sets. The first problem is tritium disposal before 1962 was reported as an annual average and the disposal data after 1962 suggest there may have been significant monthly variation in tritium disposal. The second problem is the highest observed tritium concentration in wells nearest the injection well (USGS-47, USGS-43, and USGS-41) occurs in 1962, while the disposal history indicates very little tritium was disposed of during this time. Given the close proximity of these wells to the CPP-3 injection well and relatively high aquifer velocity, tritium disposal spikes should be almost immediately seen in the nearest downgradient wells.

Figure B-15 illustrates the simulated and observed tritium breakthrough for each calibration well. The current model's RMAD error was 1.53 and the average correlation coefficient was 0.369 for all wells.

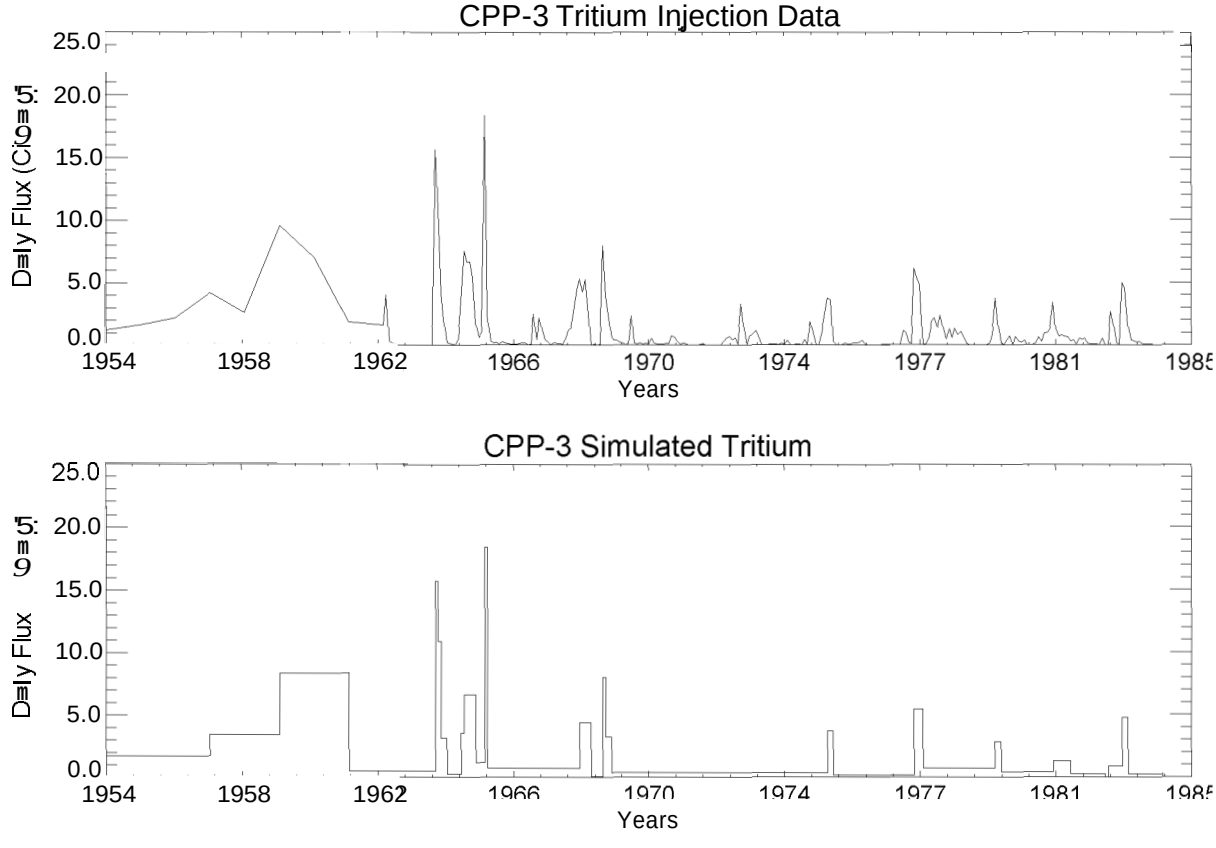

Figure B-12. The CPP-3 injection well recorded and simulated tritium disposal data.

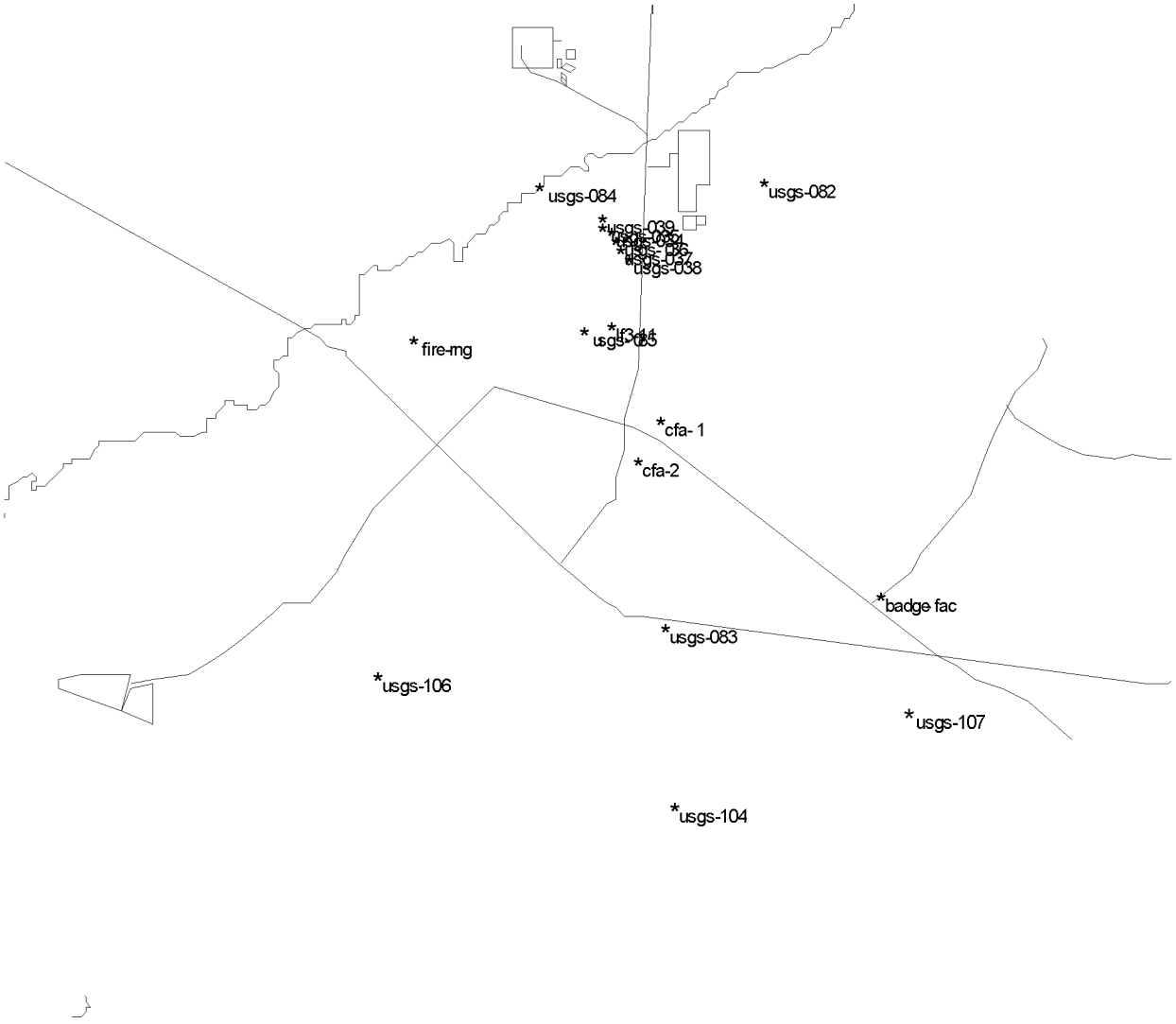

Figure B-13. Locations of tritium calibration wells.

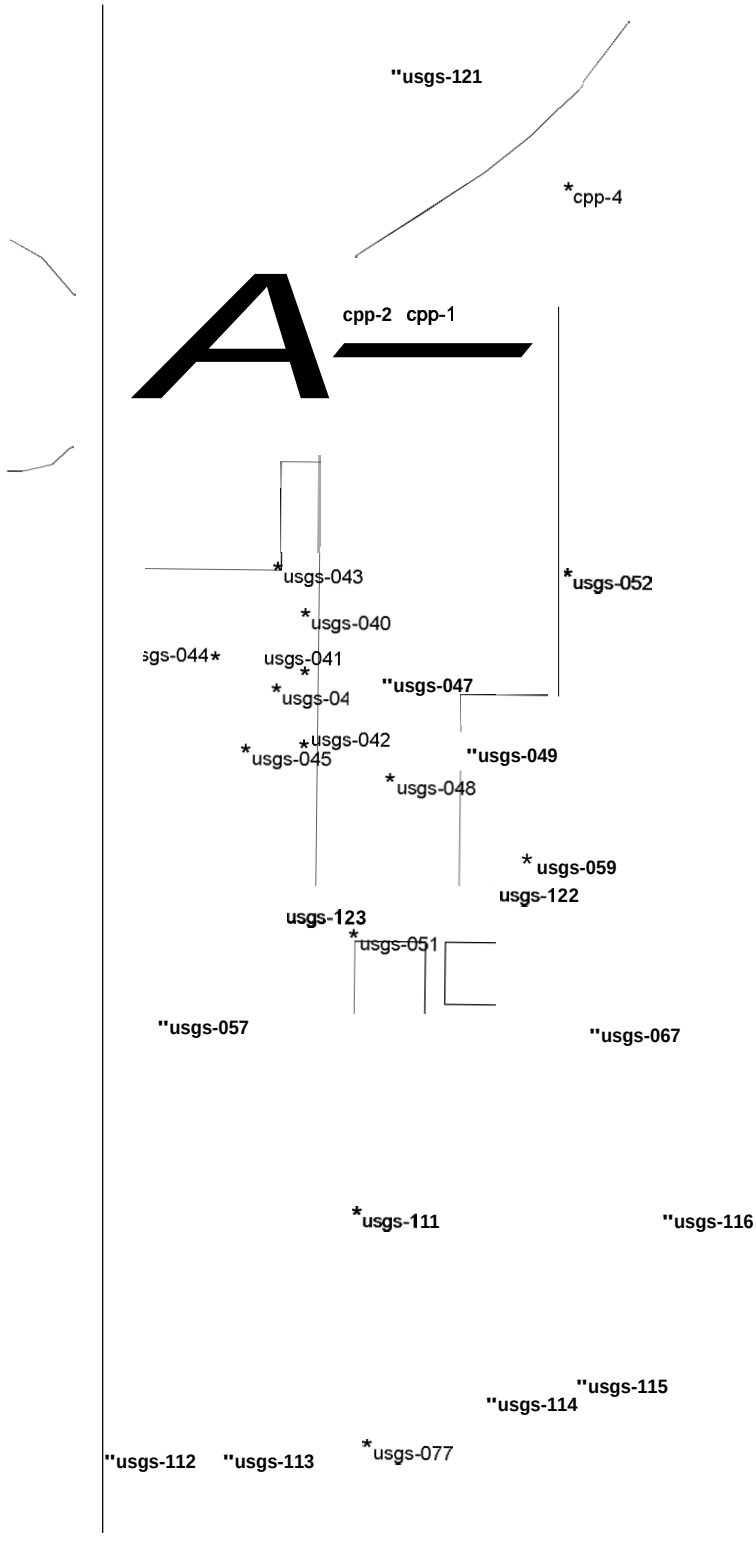

Figure B-14. Locations of tritium calibration wells near INTEC

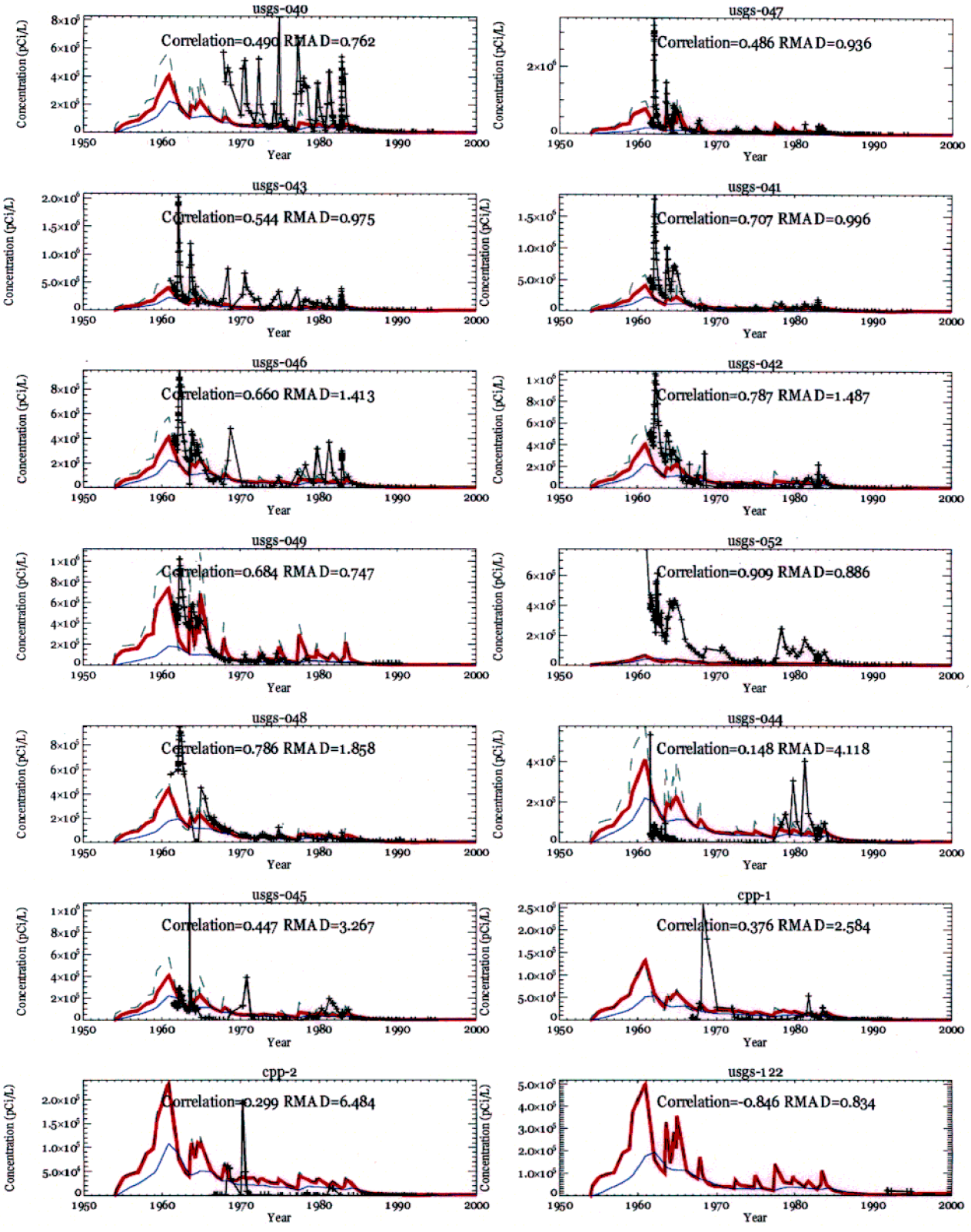

Figure B-15. *Current* model tritium calibration wells breakthrough.

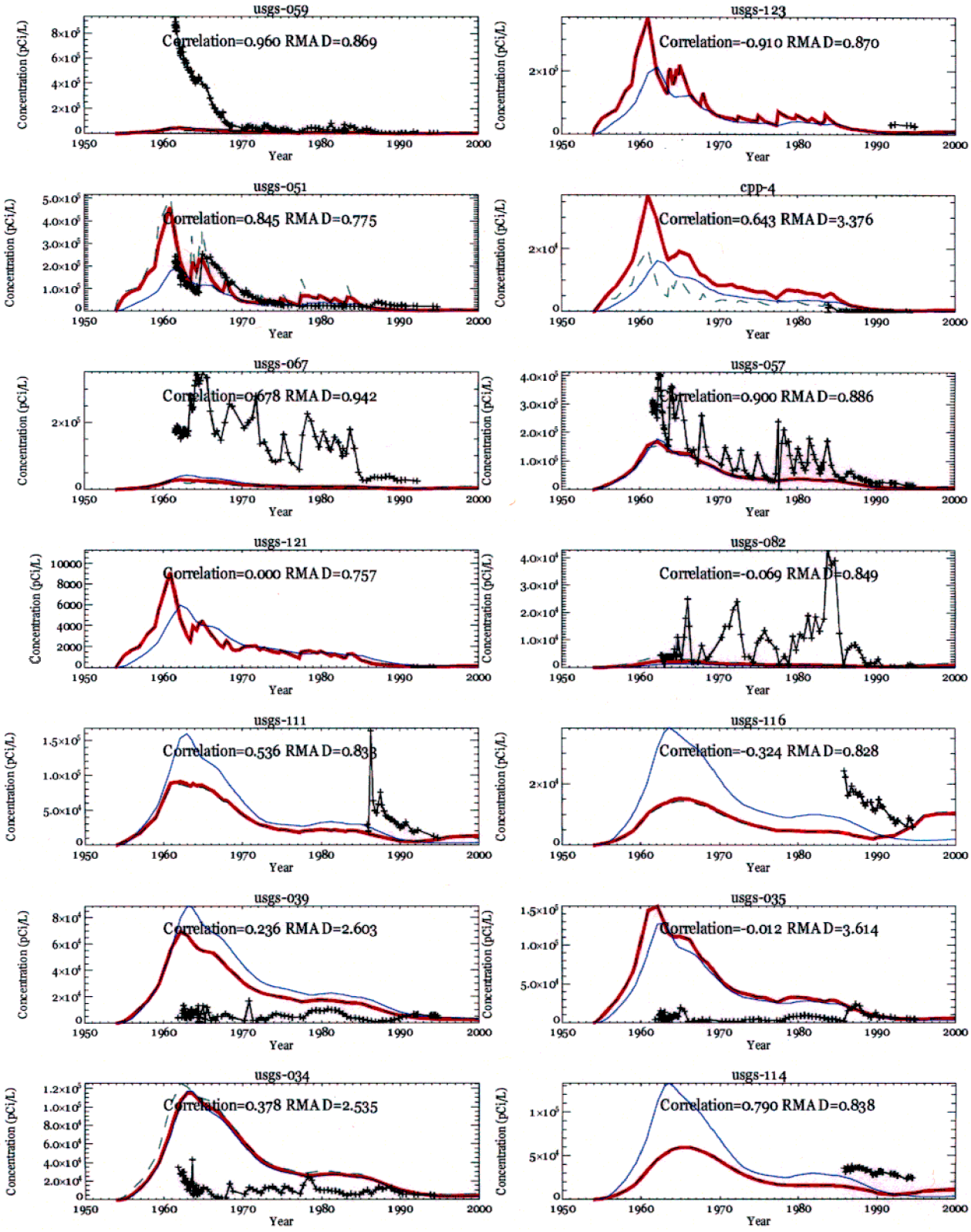

Figure B-16. Current model tritium calibration wells breakthrough.

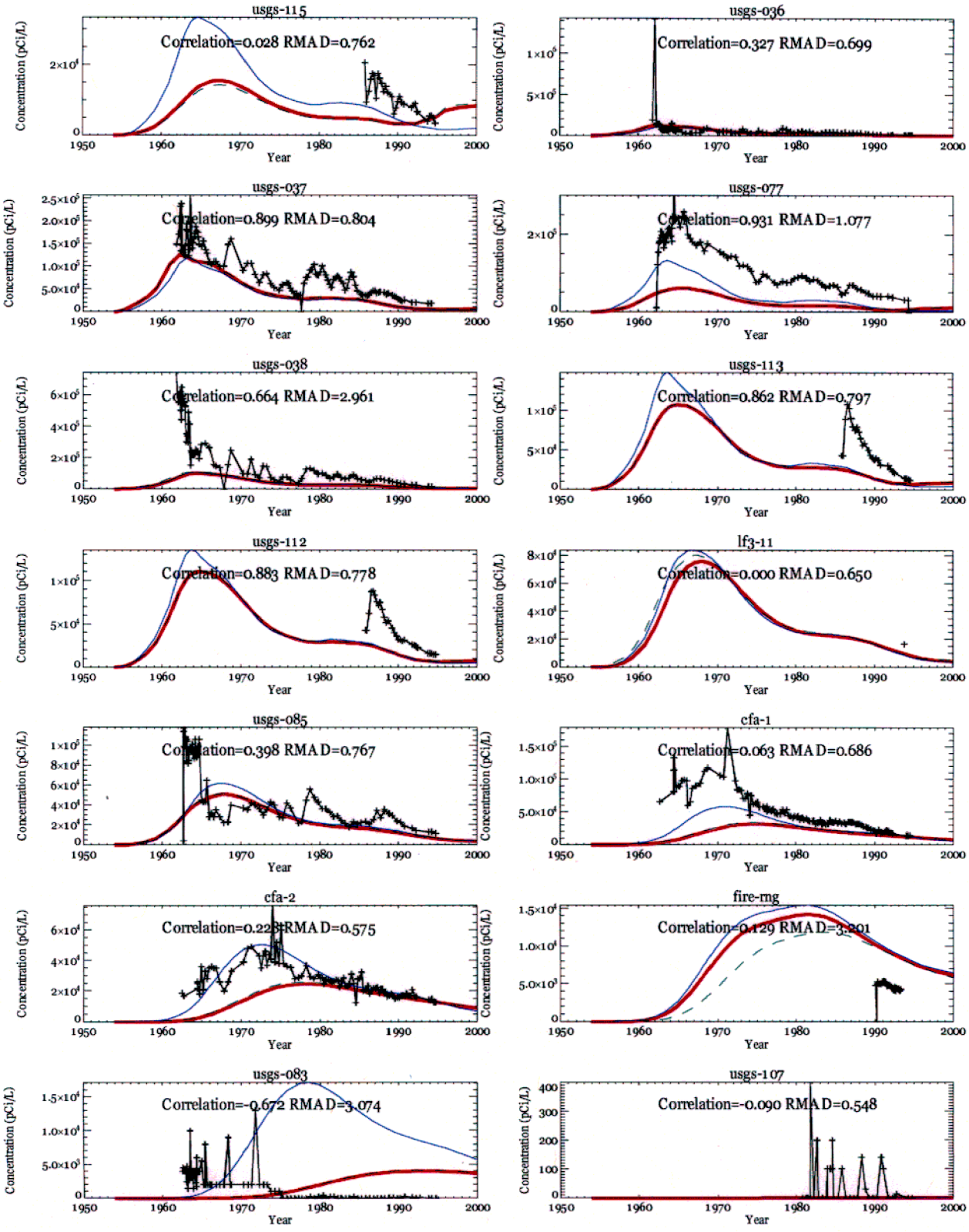

Figure B-17. Current model tritium calibration wells breakthrough.

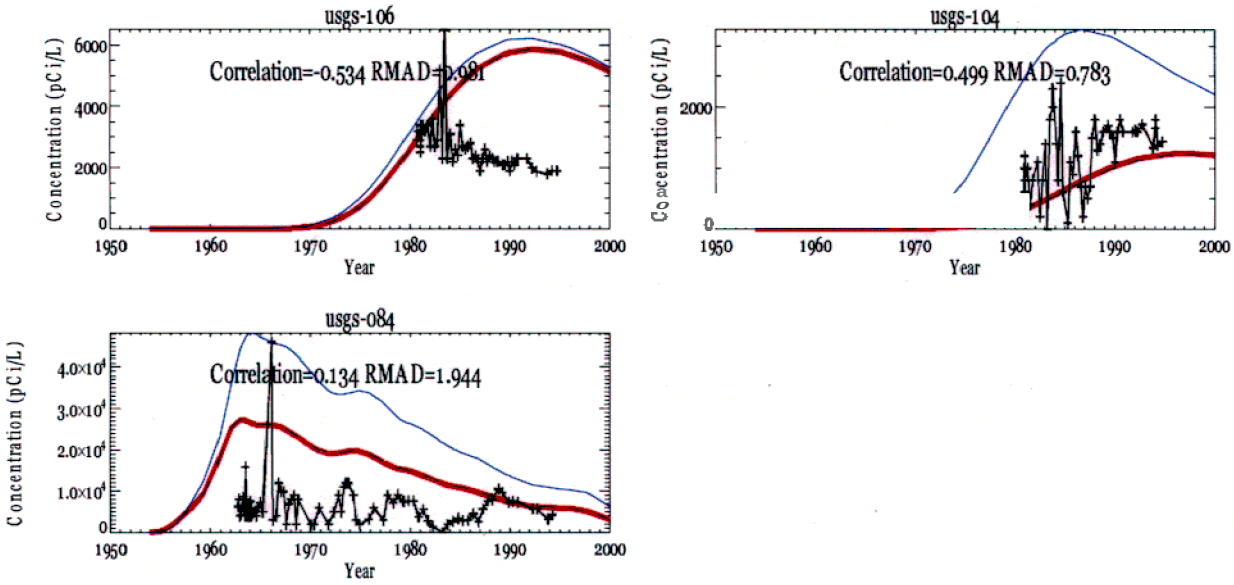

Figure B-18. Current model tritium calibration wells breakthrough.

B-3. CURRENT MODEL PREDICTIVE SIMULATIONS

The contaminants with substantial aquifer plumes migrating from INTEC were simulated with the current model. The simulated contaminants included 1-129, H-3, Tc-99, and Sr-90. Table B-3 lists each contaminant, the half-life, the partition coefficients (K_d), and the federal drinking water standard (maximum contaminant level). The partition coefficients of the contaminants that react with the subsurface (Sr-90 and Tc-99) were adjusted to better match the observed plumes. The simulations used the WAG 3, OU 3-13, and RI/BRA vadose zone simulations as the upper boundary condition. The tritium flux rate was adjusted to match vertical concentrations measured downgradient in the vertical profile boreholes. This upper boundary condition represents water flow from the vadose zone and contaminant flux from soil contamination, Tank Farm releases, and the CPP-3 injection well during the period it failed and discharged to the vadose zone.

Table ·3 Predictive simulation contaminant parameters

Contaminant	Half-life (years)	Sediment K_d (ml/g)	Basalt K_d (ml/g)	Federal Drinking Water Standard" (pCi/L)
1-129	1.57E+7	0	0	1.0
Tritium (H-3)	12.3	0	0	20,000
Sr-90	29.1	6	0.1	8
Tc-99	2.11E+5	0.075	0.0013	900

a. Based on the National Interim Primary Drinking Water Regulations, EPA-570/9-76-003.

The tritium flux rate needed to be adjusted because the current tritium concentrations in the aquifer near INTEC are most likely the result of continuing contaminant sources from INTEC vadose zone, and the RI/BRA vadose zone model poorly represents the INTEC vadose zone. Simulations of the INTEC large-scale tracer test performed in 2000 using the OU 3-13 RI/BRA vadose zone model (INEEL 2003) indicated that the effective interbeds poorly represent the actual system and the tracer was able to move much faster than the simulated tracer. Furthermore, geochemical analysis of perched water and disposal pond water (DOE-ID 2002) indicated that the disposal pond water did not move as far laterally as the OU 3-13, RI/BRA model predicted. These discrepancies between the observed and the OU 3-13 RI/BRA vadose model simulated conditions indicate the RI/BRA boundary condition is an uncertain model input, which may need to be adjusted in the aquifer model update.

The injection well 1-129 source was thought to be conservatively over-estimated in the OU 3-13 RI/BRA modeling and was reevaluated in the current modeling. The current model's predictive simulations are discussed in Sections B-3.1 through B-3.4.

B-3.1 Iodine-129

The OU 3-13 RI/BRA 1-129 source consisted of 1.52 curies and was divided between 91.6% injection well, 5% percolation ponds, and 3% other sources. The 1-129 discharge data to the CPP-3 injection well were only reported from 1976 through 1985 and the RI/BRA model's injection well 1-129 source was extrapolated before 1976. The RI/BRA I-129 source over-predicted current concentrations observed in the aquifer.

The injection well source was reduced from 1.39 Ci to 0.86 Ci based on analysis of the historical INTEC processes and the need to better match current aquifer concentrations. A full explanation of the revised 1-129 source term is presented in Section 4 of the main report.

Perched water concentrations that may be the result of the injection well collapse and subsequent discharge to the vadose zone also might suggest that the early RI/BRA 1-129 source might have been over-estimated. The average I-129 concentration using the RI/BRA source was approximately 30 pCi/L during the reported period. This value was calculated from the average disposal rate of 1.2×10^8 pCi/day in 4,000 m^3/day of injection water (DOE-ID 1997). The deep perched water near the injection should be near this concentration, if significant water is not moving through the perched water and the RI/BRA 1-129 source is accurate. However, sampling of the nearest deep perched water sampling location (USGS-50) to the CPP-3 injection well detected 1-129 at 0.65 pCi/L (DOE-ID 2002), suggesting that the I-129 source strength might have been significantly overestimated.

The 1-129 concentrations simulated by current model with the new source term exceeded the maximum contaminant level through the year 2060. The simulated 2001 peak 1-129 concentration was 3.0 pCi/L and was located approximately 400 m west of the Central Facilities Area (CFA). This hot spot is the result of injection well operation. The peak measured 1-129 concentration during 2001 sampling was 1.06 pCi/L in Well LF-08, which is located approximately 1,000 m northwest of the CFA. The simulated 2095 peak 1-129 concentration was 0.5 pCi/L and was located south of INTEC near the southern INEEL boundary. The much higher simulated than observed 1-129 concentrations in 2001 suggest the revised source term discussed in Section 4 may still be over-estimating the 1-129 source. Figures B-19 through B-22 illustrate simulated I-129 peak aquifer concentration, horizontal concentrations in 2001, vertical concentrations in 2003, and simulated with observed in the vertical profile boreholes in 2003, respectively. The observed I-129 concentrations from 2001 sampling is illustrated in Figure B-23.

The CFA-1 and CFA-2 production wells have historically produced approximately 250,000 gal/day and the wells were included in the aquifer simulations. The total 1-129 produced from these two water-supply wells for the period 1954 through 2003 was only 0.01 curies. This value is only a small fraction of the total 1-129 injection well inventory, because the 1-129 plume is very dilute at the production well locations. The model indicates the wells do not capture a significant portion of the 1-129 plume.

It appears that the current 1-129 contamination in the aquifer near INTEC is derived primarily from 1-129 discharged in the percolation ponds and 1-129 that entered the vadose zone during the injection well collapse that is slowly migrating to the aquifer. The 1-129 resulting from the injection well should have moved far south of the INTEC facility by this time, because of the fast aquifer velocity (approximately 2 m/day) and because regular injection well operation ceased in 1984. However, very low permeability and localized basalt formations near INTEC could be slowly releasing 1-129 under the natural gradient. The groundwater mound resulting from the injection well operation most likely produced an artificial gradient, which may have moved contaminants in the lower permeability basalt relatively quickly compared to their release under the natural gradient. Approximately 7% of the total 1-129 source was discharged to the percolation ponds and the injection well during the well collapse period. The 1-129 concentrations should decrease in the hture as the vadose zone sources are depleted.

Simulated I-129 concentrations were higher than those observed. Aquifer sampling performed measured I-129 concentrations below the MCL at all measurement locations. The difference between simulated and measured 1-129 concentrations might be due to over-estimation of the 1-129 source term or some unknown attenuation mechanism such as adsorption, which is not considered in the current conceptual and numerical model as reducing concentrations.

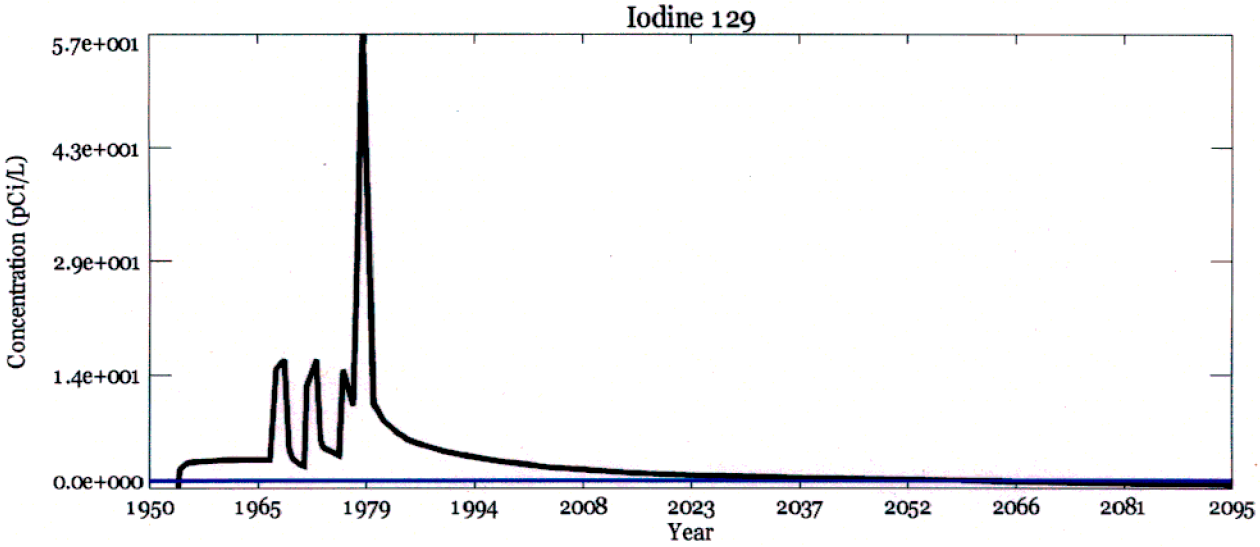

Figure B-19. Simulated I-129 peak aquifer concentrations (the blue line is the MCL).

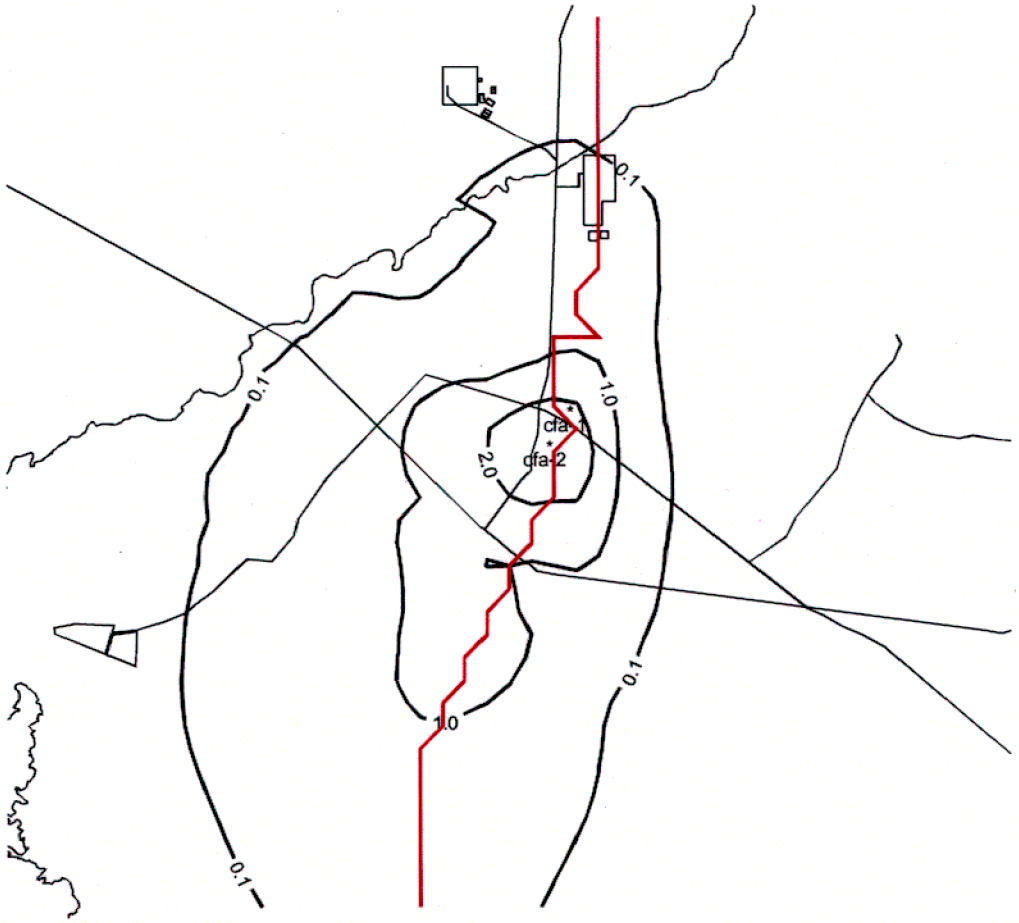

Figure B-20. Simulated I-129 (pCi/L) concentrations at the water table in 2001 (the thick red line is a fence diagram cross-section for Figure 8-21).

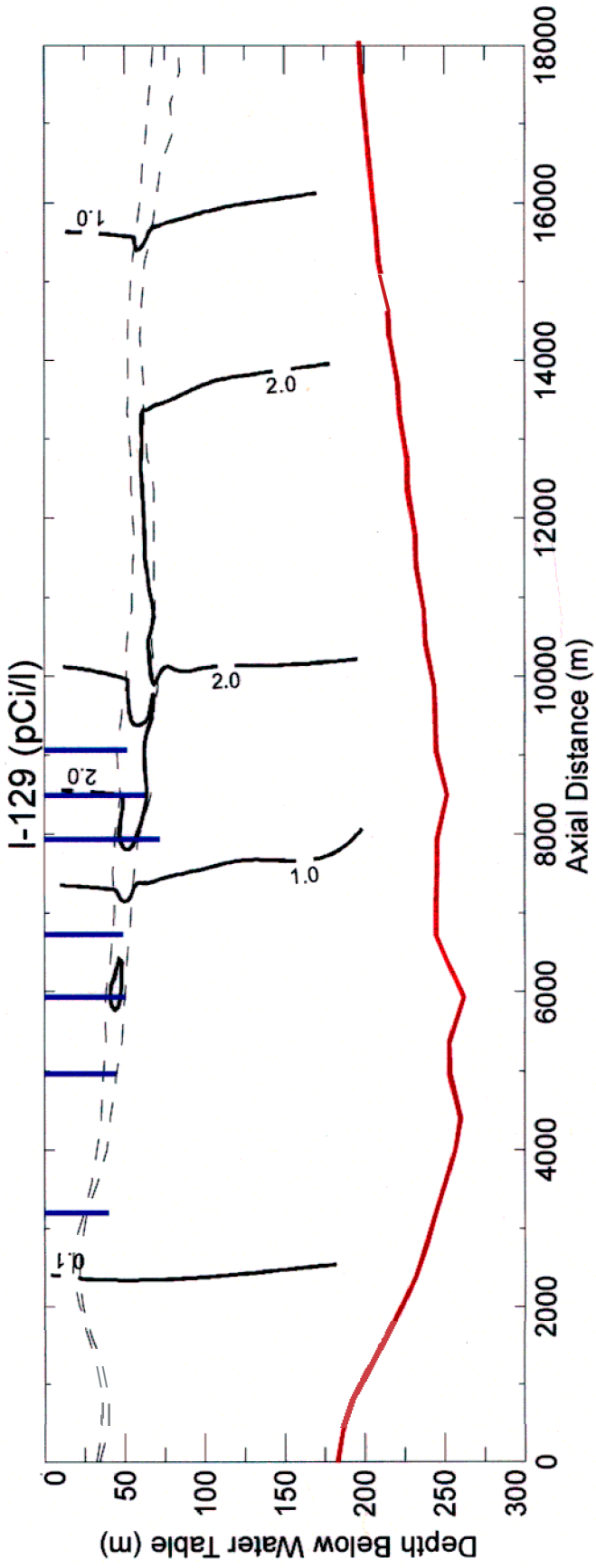

Figure B-21. Simulated I-129 vertical concentrations in 2003 (blue lines are well locations and red line is aquifer bottom).

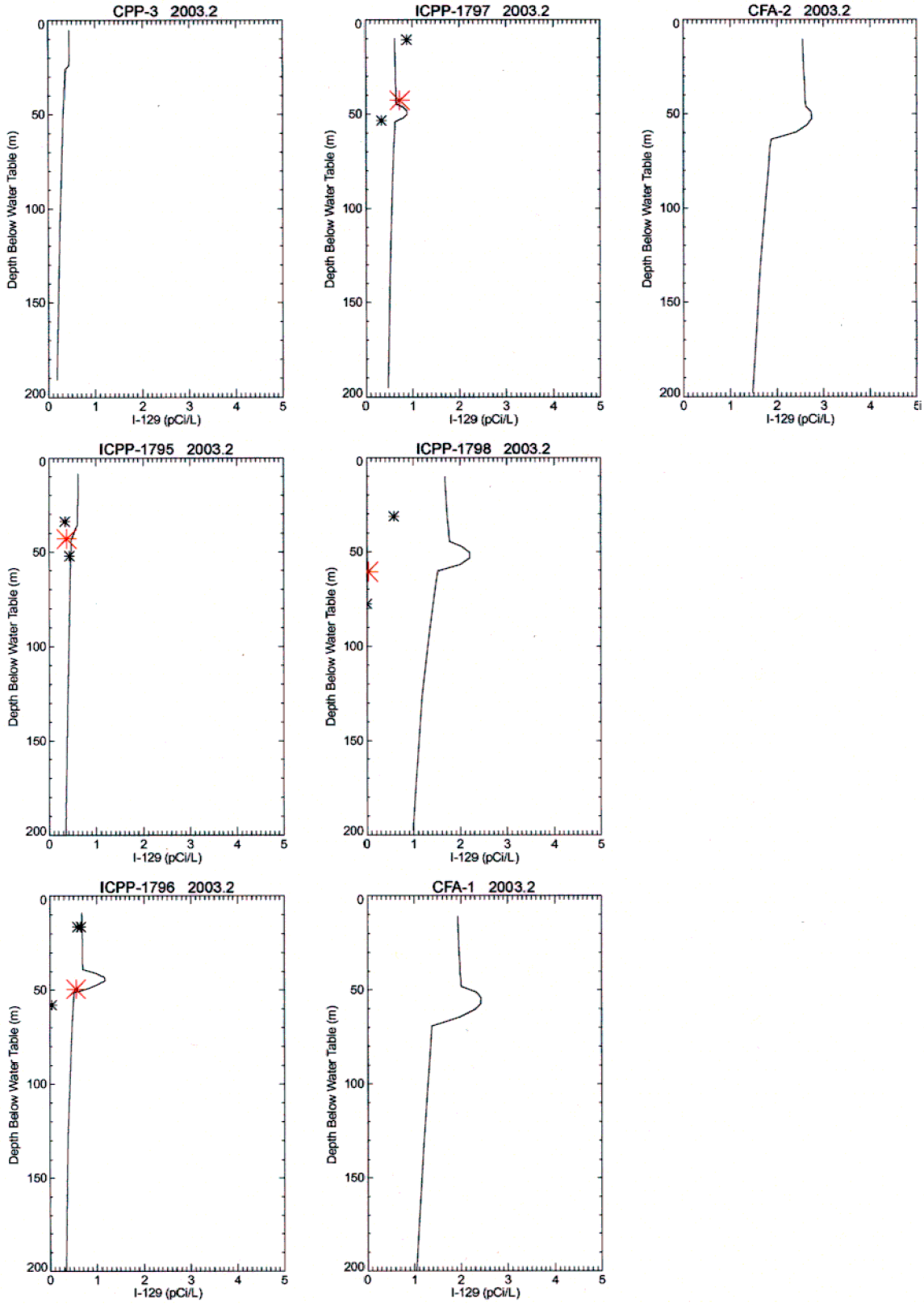

Figure B-22. Simulated I-129 versus measured concentrations at vertical boreholes in 2003 (the solid line is simulated, small asterisk is measured basalt, and large asterisk is measured HI interbed).

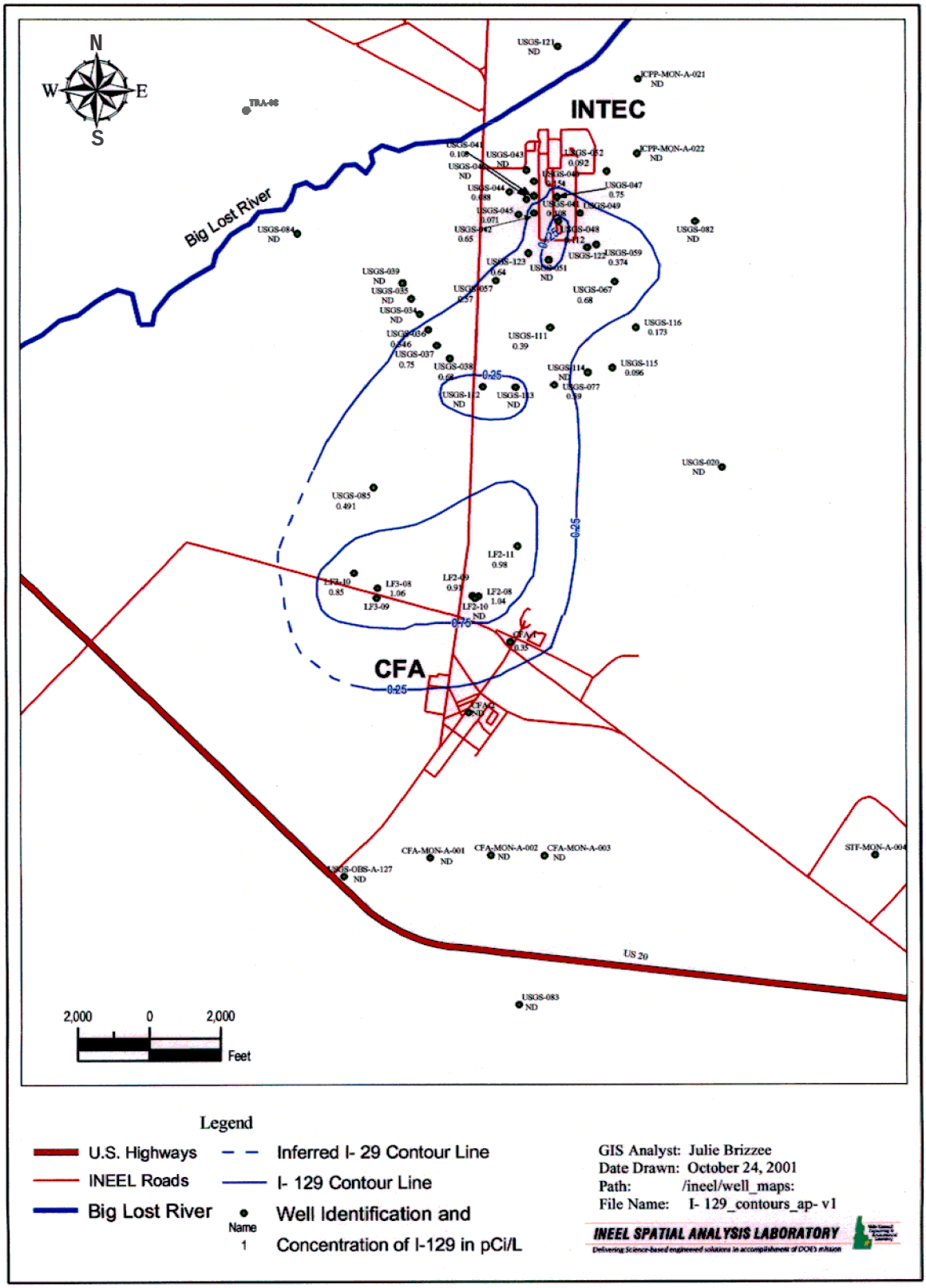

Figure B-23. Observed I-129 aquifer concentrations in 2001.

B-3.2 Tritium

The OU 3-13 RI/BRA tritium source consisted of 30,400 curies of which 71% is from the INTEC area and 29% is from TRA. The 71% from the INTEC area is 66% injection well, 3% percolation ponds, and 2% other sources. The current model's vadose zone tritium flux was increased by a factor of 2.5 to match observed concentrations in the vertical profile boreholes. The increase represents 1,305 Ci out of 21,495 Ci total tritium released into the lithosphere from INTEC operations or 1,305 Ci out of 2,104 Ci total tritium released to the INTEC vadose zone. The increased vadose zone flux did not increase the total vadose zone tritium sources to the aquifer beyond 2,104 Ci during the 1954 through 2003 simulation period.

Tritium concentrations exceeded the 10^{-6} risk concentrations throughout the 1954 to 2003 simulation period and exceeded the maximum contaminant level through the year 1999. The simulated 2001 peak tritium concentration that was not associated with the TRA tritium plume was 13,905 pCi/L and was located 400 m south of the former percolation ponds. The peak tritium concentration measured during 2001 sampling was 14,000 pCi/L in USGS-114, which is located approximately 900 m south of the former percolation ponds. The tritium simulation was not performed beyond **2003** because of uncertainty in the vadose zone flux boundary condition, which needs to be better understood for predictive modeling. Figures B-24 through B-27 illustrate simulated tritium peak aquifer concentration, horizontal concentrations at the water table in 2001, vertical concentrations in 2003, and simulated with observed in the vertical profile boreholes in 2003, respectively. The observed tritium concentrations from 2001 sampling is illustrated in Figure B-28. Simulated horizontal concentrations are presented for 2001, because the last round of complete aquifer sampling was performed in 2001 and these observations provided the best data set for model comparison.

The simulated and observed tritium plumes are different because the observed plume was estimated without using TRA tritium data and assuming the current plume is disconnected from the historical plume south of the CFA. Tritium concentrations south of the CFA in Wells USGS-104 and USGS-106 were approximately 1,000 pCi/L in 2003. These observations are still less than model predictions, but indicate tritium originating from the INTEC is still observable south of the CFA.

The tritium vertical sampling suggests the HI interbed may be acting as a confining layer between the deep and shallow aquifer, but concentrations are not as different as the earlier modeling indicated. Concentrations in the vertically sampled wells were higher than the model predicted without adjusting the vadose zone source term. This indicates there is a greater continuing tritium source from the aquifer than the OU 3-13, RI/BRA vadose zone model predicted. This increased vadose zone tritium flux may be due to the RVBRA model under-predicting the rate tritium can migrate from the vadose zone or from additional tritium and unknown tritium releases.

The current tritium contamination in the aquifer near INTEC is most likely from tritium discharged in the percolation ponds and tritium that entered the vadose zone during the injection well collapse. Approximately 16% of the total non-TRA tritium source was discharged to the percolation ponds and the injection well during the well collapse period. Tritium concentrations should decrease in the near future as vadose zone sources are depleted and radioactive decay reduces the amount of tritium in the vadose zone. The decline in tritium aquifer concentrations should be faster than the 1-129 concentrations because of radioactive decay.

The model predicts tritium from INTEC is widespread far south of the CFA. However, the current very low contaminant concentrations in Well USGS-83 are not consistent with the current model. The current nondetect tritium concentration in this well is most likely an anomaly, because tritium sampling performed by WAG 4 in 2000 detected tritium in USGS-104 at 1,050 pCi/L and in USGS-106 at

1,110 pCi/L, which is more consistent with the model. Well USGS-104 is located approximately 3 km south of Highway 20 in a direction south of INTEC, and USGS-106 is located midway between the junction of Highway 20 and Lincoln Boulevard, and the Subsurface Disposal Area.

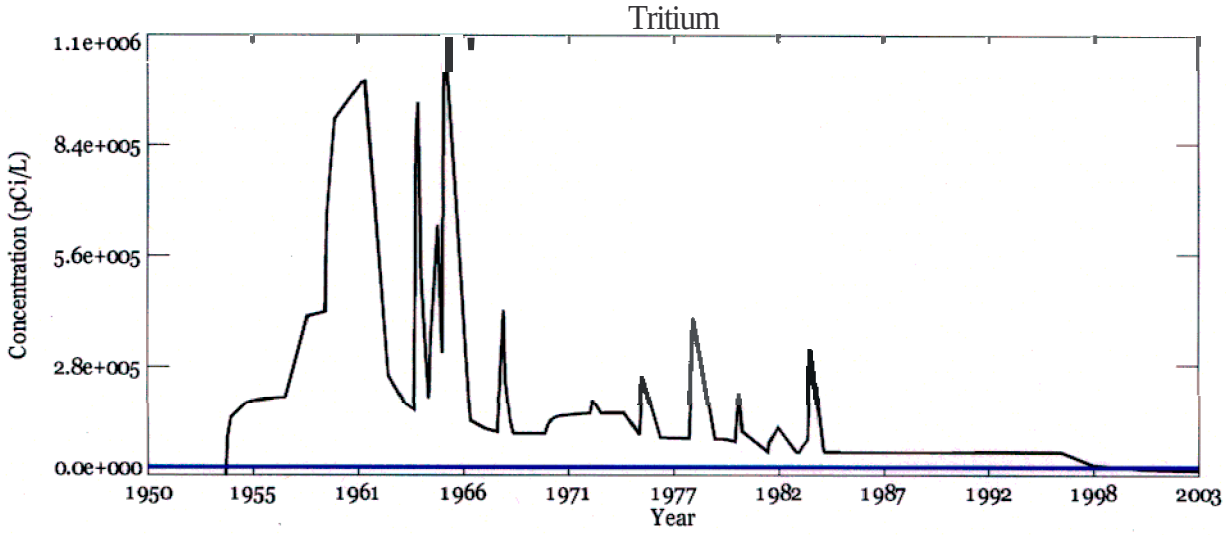

Figure B-24. Simulated tritium (pCi/L) peak aquifer concentrations (the blue line is the MCL).

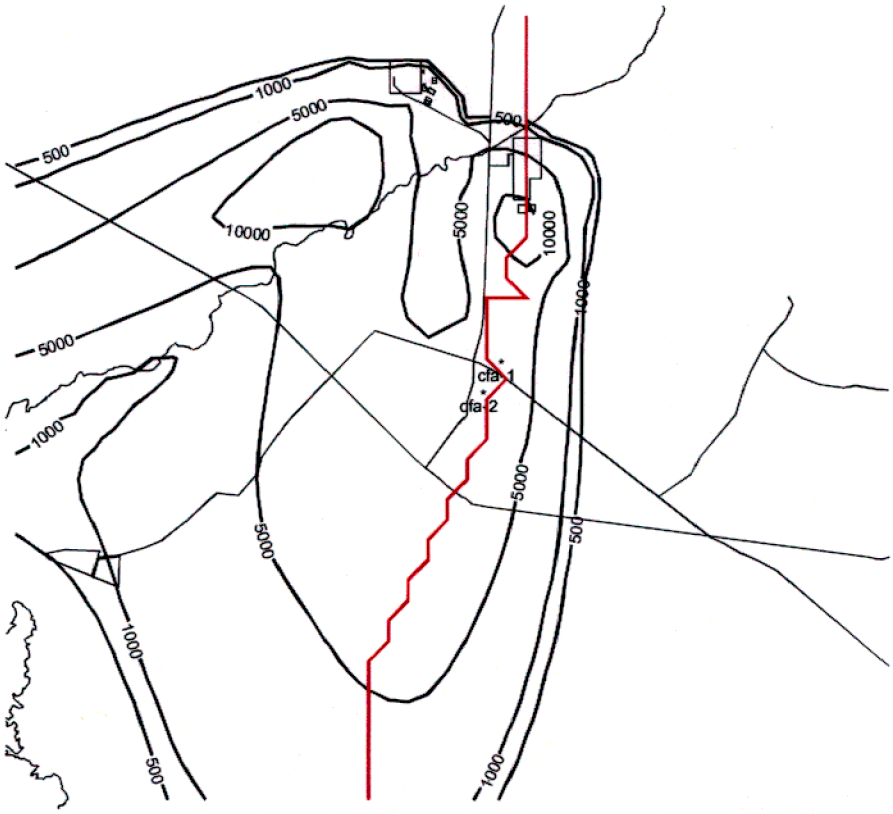

Figure B-25. Simulated tritium (pCi/L) concentrations at the water table in 2001 (the thick red line is a fence diagram cross-section for Figure B-26).

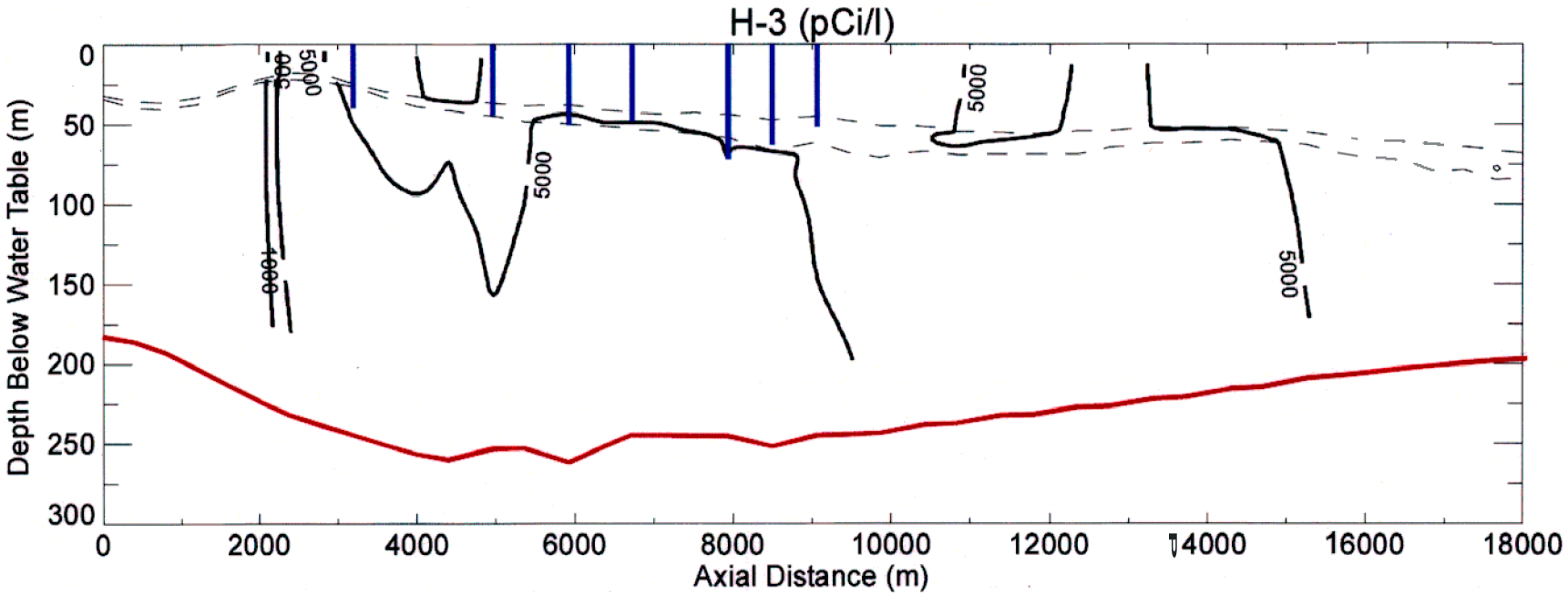

Figure B-26. Simulated tritium vertical concentrations in 2003 (the blue lines are well locations and red line is aquifer bottom).

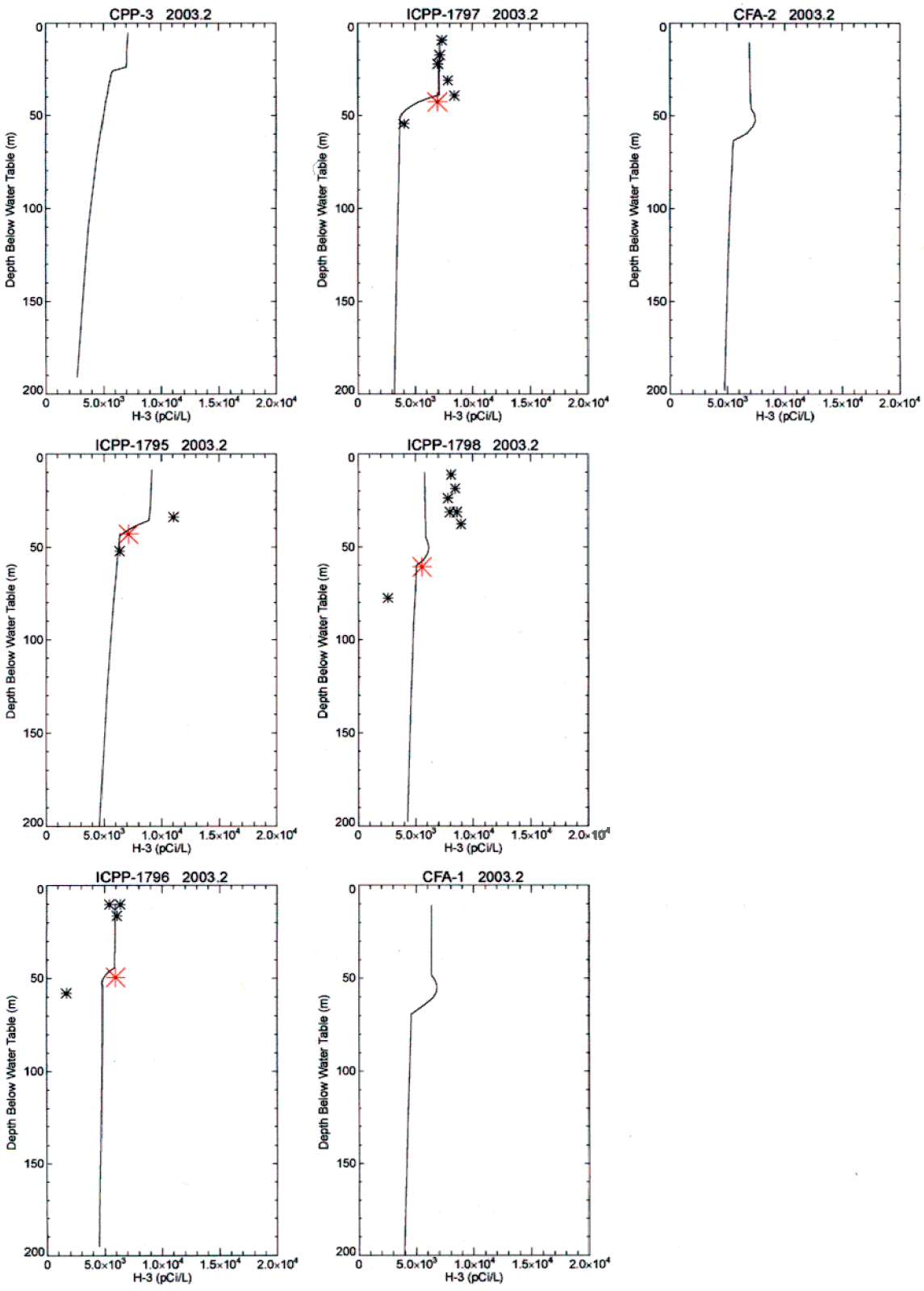

Figure B-27. Simulated tritium versus measured concentrations at vertical boreholes in 2003 (the solid line is simulated, the small asterisk is measured basalt, and the large asterisk is measured HI interbed).

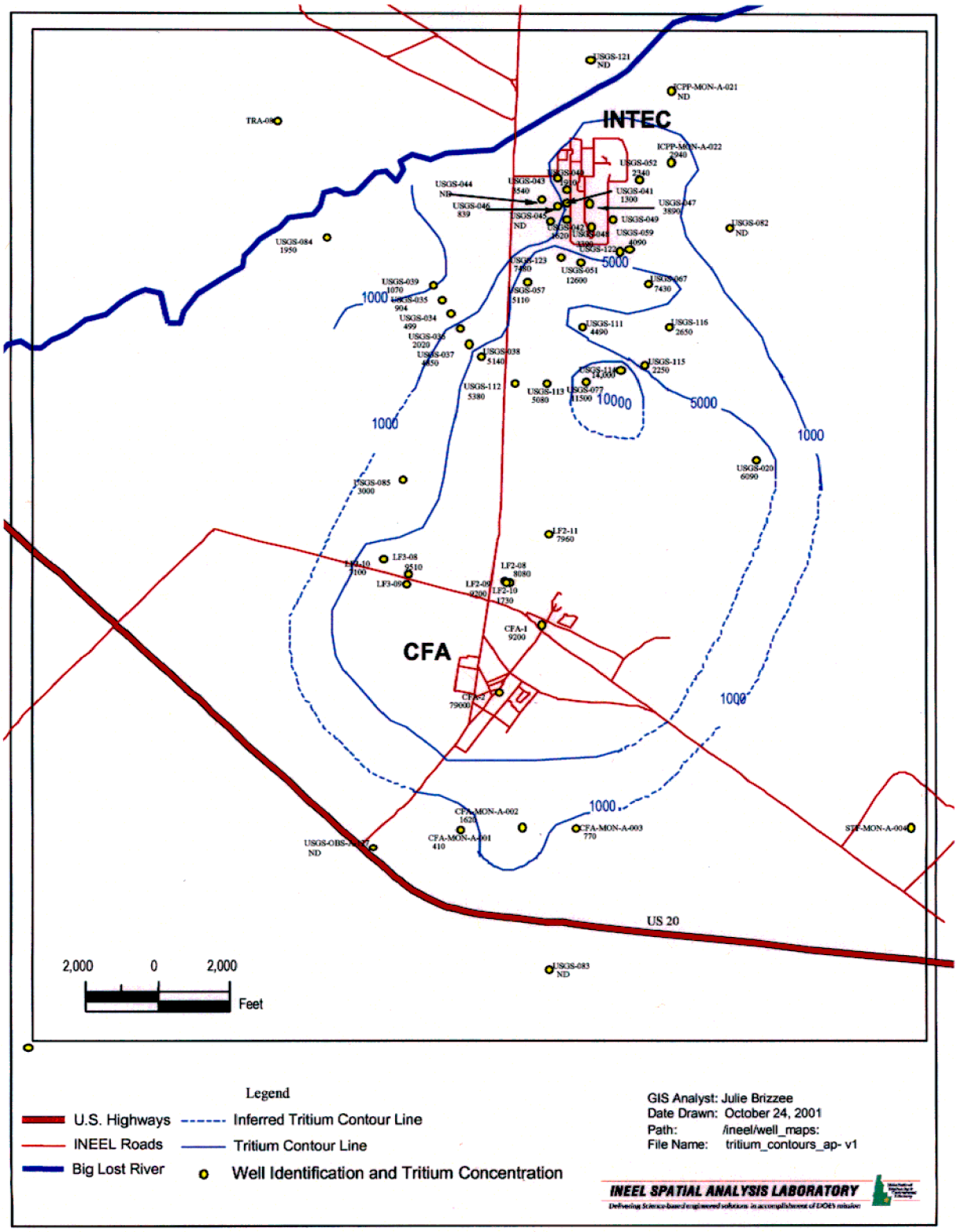

Figure B-28. Observed tritium aquifer concentrations in 2001.

B-3.3 Technetium-99

The OU 3-13, RI/BRA Tc-99 source consisted of 2.69 curies and is divided between 96% Tank Farm and 4% soil contamination. No significant amounts of Tc-99 were released into the injection well or percolation ponds. The current model under-predicted concentrations in the vertical profile boreholes. Increasing the Tc-99 vadose zone flux improved the agreement with concentrations in the vertical profile boreholes, but increasing the vadose flux by the same 2.5 factor used in the tritium simulations over-estimated the Tc-99 source by a factor 1.8 over the RI/BRA total source; therefore, this simulation was rejected.

The total Tc-99 source term was most certainly under-estimated in the RI/BRA modeling, because no Tc-99 was reported released to the injection well. Historically, Tc-99 has been observed far south of the INTEC, suggesting Tc-99 was released into the injection well. The Tc-99 source term will need to be reevaluated with the planned update of the Group 4 vadose zone model.

Reducing the current model's basalt K_d value from 0.006 to 0.0013 and the interbed K_d value from 0.15 to 0.075 improved the agreement with the observations. The interbed K_d was reduced by a factor of 2 from that used in the RI/BRA modeling and the basalt K_d was 1/60 of the interbed value. In contrast to the tritium concentrations, the Tc-99 concentrations do not indicate concentrations are substantially different above, within, or below the interbed. Figures B-29 through B-32 illustrate simulated Tc-99 peak aquifer concentration, horizontal concentrations at the water table in 2001, vertical concentrations in 2003, and simulated with observed in the vertical profile boreholes in 2003, respectively. The observed Tc-99 concentrations from 2001 sampling is illustrated in Figure B-33.

Simulated Tc-99 concentrations were significantly under-predicted in the vertical profile boreholes, which might be due to the RI/BRA model over-predicting spreading in the vadose zone, thereby resulting in a vadose zone contamination footprint that is larger than that observed. The RI/BRA vadose zone model footprint extended approximately 700 m beyond the INTEC fence line in the east, west, and north directions and 1,100 m beyond the INTEC fence line in the south direction, even west of the Big Lost River near TRA. The RI/BRA vadose zone model predicted contaminants would spread extensively in the horizontal direction. This resulted in the current model over-estimating the aquifer contamination in directions lateral and upgradient to the aquifer flow and under-estimating peak aquifer concentrations directly beneath and downgradient of INTEC.

Simulated Tc-99 concentrations never exceeded the MCL throughout the 1954 through 2003 simulation period. The Tc-99 simulation was not performed beyond 2003 because of uncertainty in the vadose zone flux boundary condition, which needs to be better understood for predictive modeling. The simulated 2001 peak Tc-99 concentration was 21.5 pCi/L and was located near the northwest corner of INTEC. The observed peak Tc-99 concentration measured during 2003 was 2,840 ± 43.4 pCi/L in new SRPA Monitoring Well ICPP-MON-A-230. This well is located inside the INTEC, approximately 300 ft north of the Tank Farm's northern fence line. Because Tc-99 was detected in the aquifer at concentrations much higher than observed previously, a special investigation of the occurrence of Tc-99 at INTEC was initiated in August 2003. The final results of the Tc-99 investigation are not yet available, but will be reported in the 2004 Annual Well Monitoring Report. Preliminary results suggest that the Tc-99 appears to have been present in the SRPA beneath the northern portion of INTEC for many years. The most likely source of the Tc-99 in the groundwater in this area appears to be from past releases that occurred at the Tank Farm. The most likely mechanism for transport of Tc-99 to the aquifer is downward movement of contaminated water through the vadose zone to the water table. The former INTEC injection well likely constituted an earlier source of Tc-99 to the aquifer, but groundwater Tc-99 concentrations in the aquifer associated with the former injection well were far below the MCL. The INTEC vadose zone model will be revised in 2004 to better predict the migration of Tc-99 through the vadose zone to the aquifer.

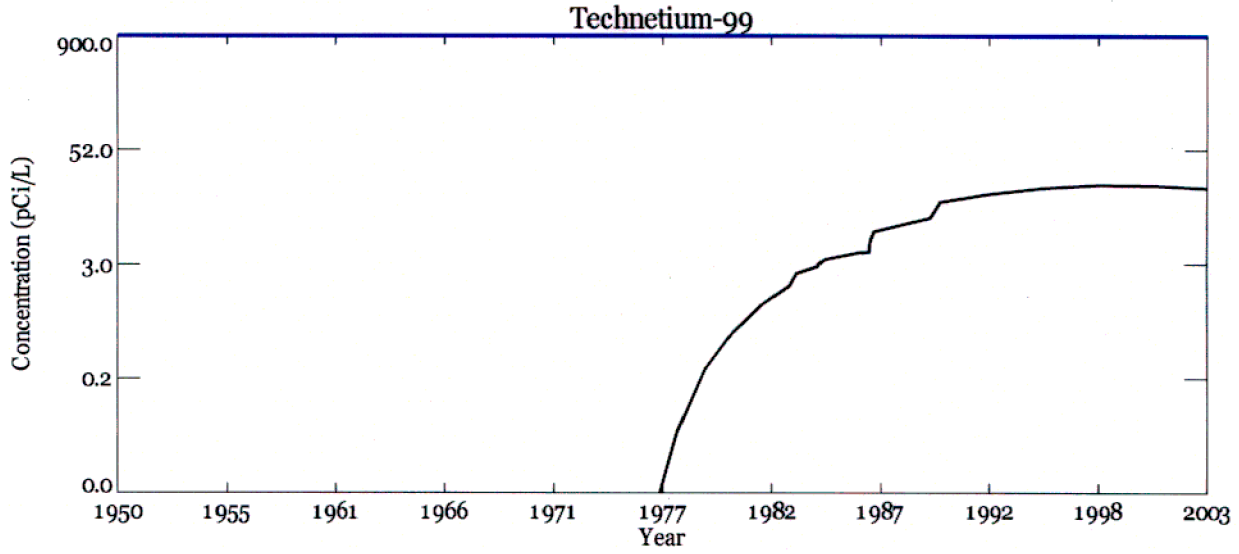

Figure B-29. Simulated Tc-99 peak aquifer concentrations (the blue line is the MCL).

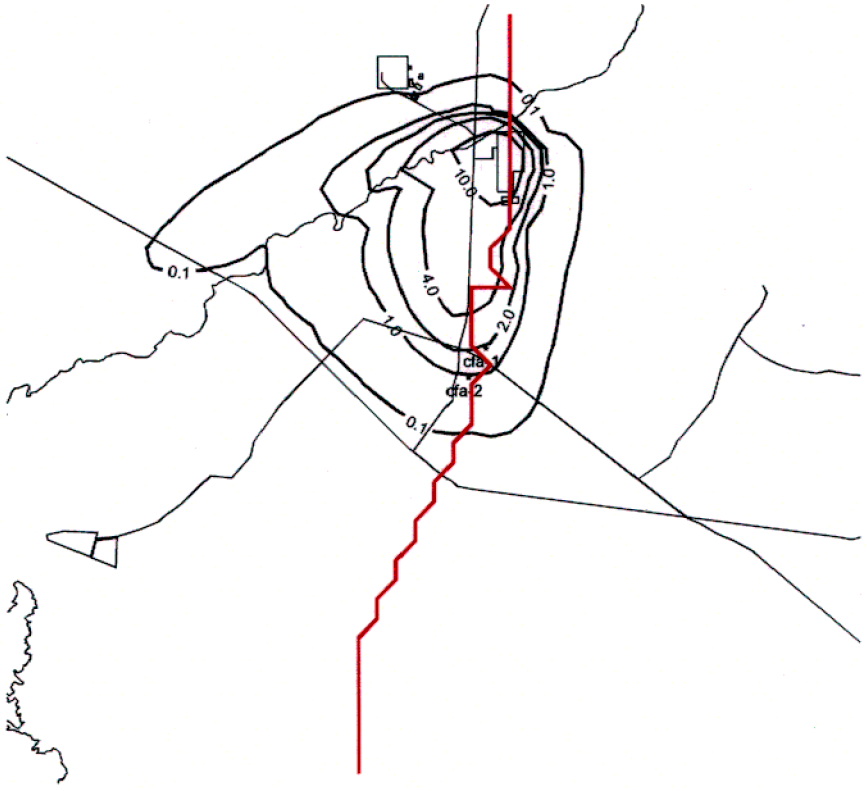

Figure B-30. Simulated Tc-99 concentrations (pCi/L) at the water table in 2001 (the thick red line is a fence diagram cross-section for Figure B-31).

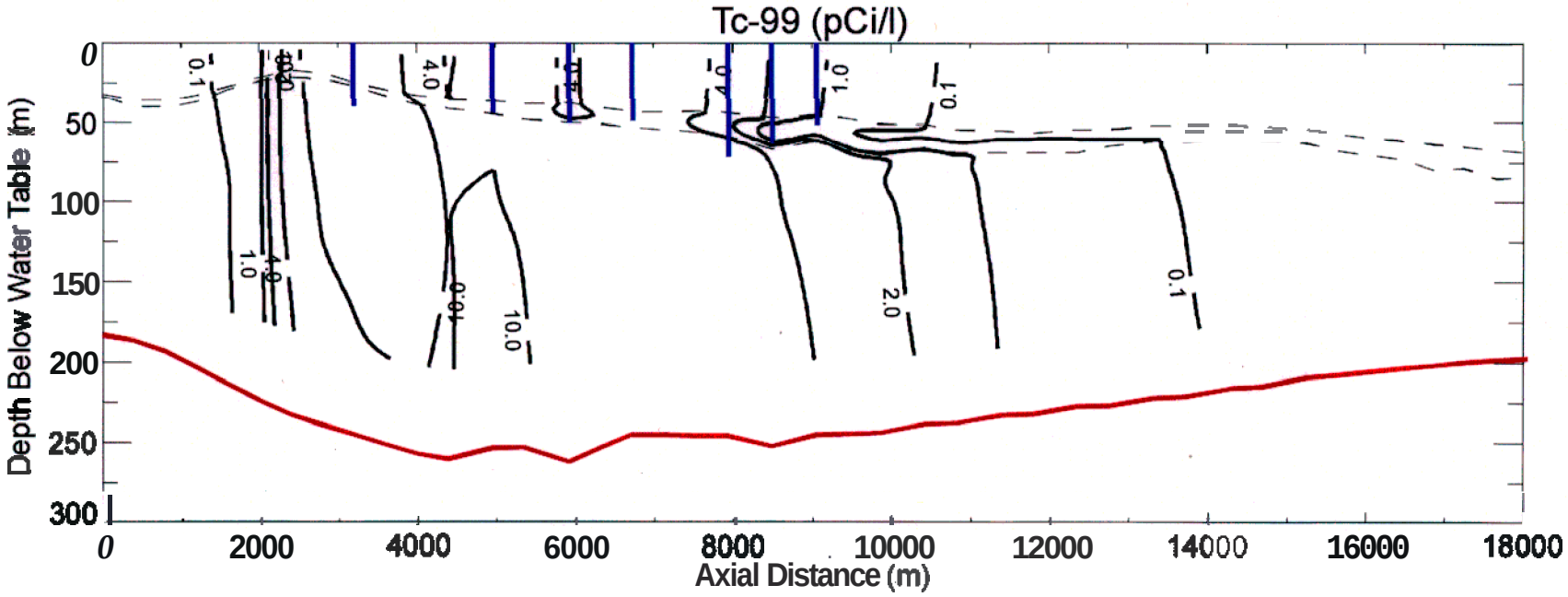

Figure B-31. Simulated Tc-99 vertical concentrations in 2003 (the blue lines are well locations and red line is aquifer bottom).

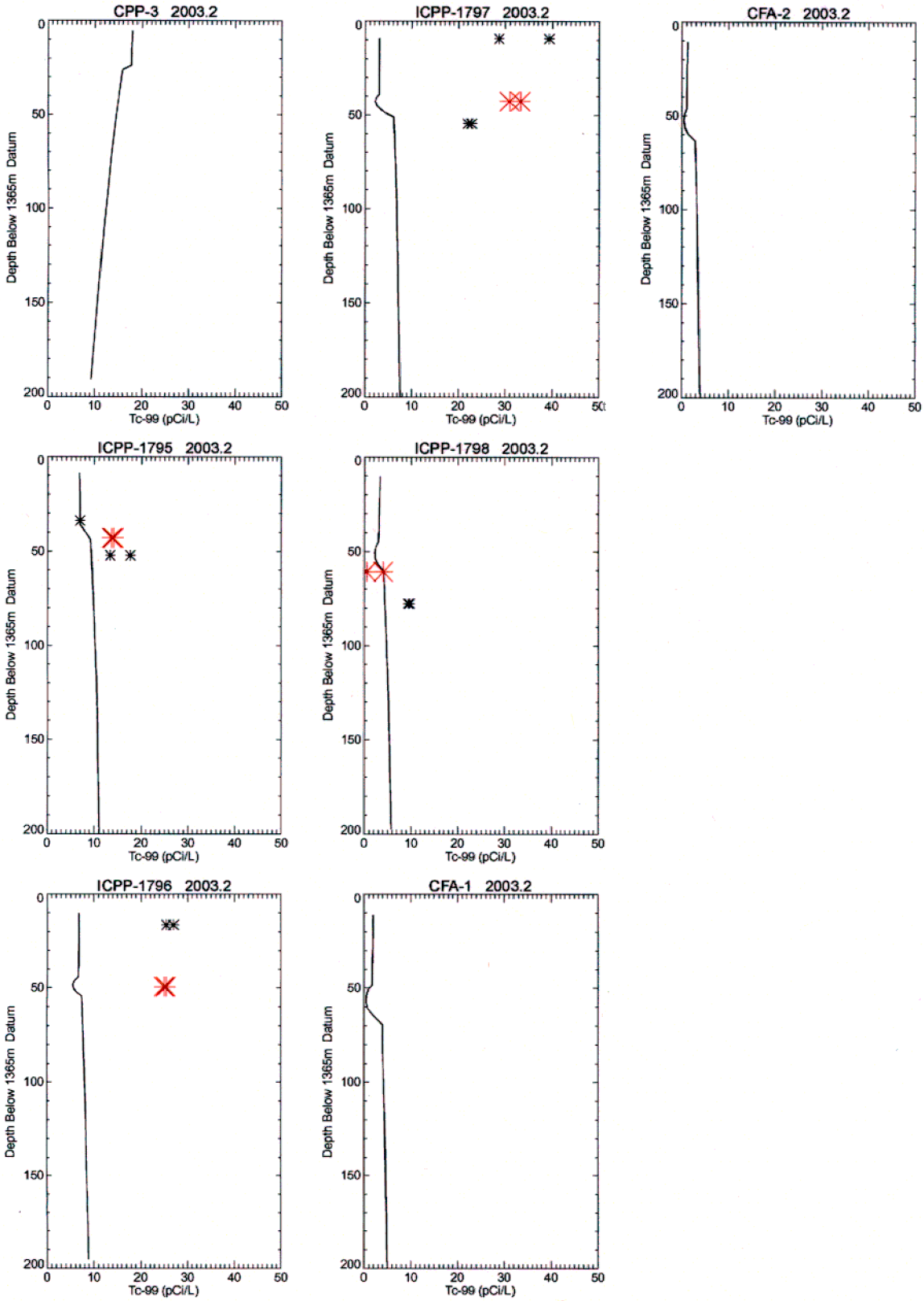

Figure B-32. Simulated Tc-99 versus measured concentrations at vertical boreholes in 2003 (the solid line is simulated, small asterisk is measured basalt, and large asterisk is measured HI interbed).

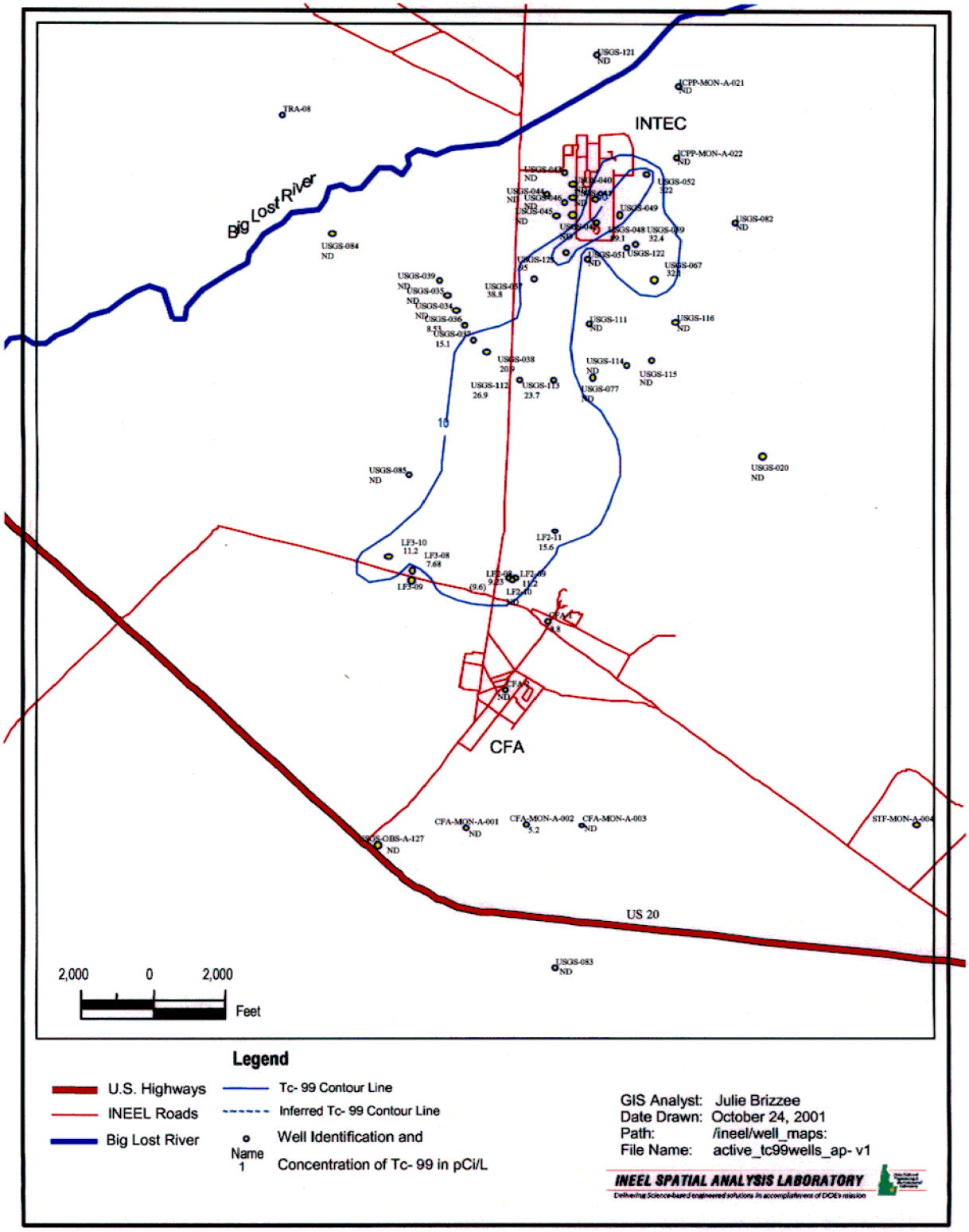

Figure B-33. Observed Tc-99 aquifer concentrations in 2001.

B-3.4 Strontium-90

The OU 3-13 RI/BRA Sr-90 source consisted of 19,400 curies and is divided between 92% Tank Farm, 6% soil contamination, 29% TRA, and 2% other sources. Increasing the Sr-90 vadose flux by a factor of 2.5 had no significant change in aquifer concentrations, because very little Sr-90 is predicted to enter the aquifer from the RI/BRA vadose zone model throughout the 1954 through 2003 simulation period. This is because Sr-90 is more strongly retarded in the vadose zone by adsorption than the other contaminants.

As with the Tc-99 simulations, better agreement with the observed Sr-90 concentrations was obtained by reducing the interbed K_d value from 12 to 6 and setting the basalt K_d to be 1/60 of the interbed value. This was needed to compensate for the larger retardation due to a higher bulk density of the current model's lower basalt porosity. This is because retardation is directly proportional to the soil's bulk density and bulk density is inversely proportional to porosity. Thus, the retardation will increase for a lower-porosity soil given the same K_d. The K_d reduction factor is the same as that used to improve the Tc-99 simulation's agreement with the observed data. As with the Tc-99 concentrations, the observed Sr-90 concentrations do not indicate concentrations are substantially different above, within, or below the interbed.

The simulated Sr-90 concentrations exceeded the maximum contaminant level throughout the 1954 through 2003 simulation period. The simulated 2001 peak Sr-90 concentration was 19.1 pCi/L and was located 400 m southwest of the former percolation ponds. The peak Sr-90 concentration measured during 2001 sampling was 26.4 pCi/L in USGS-123, which is located approximately 300 m northwest of the former percolation ponds. The Sr-90 simulation was not performed beyond 2003 because of uncertainty in the vadose zone flux boundary condition, which needs to be better understood for predictive modeling. Figures B-34 through B-37 illustrate simulated Sr-90 peak aquifer concentration, horizontal concentrations at the water table in 2001, vertical concentrations in 2003, and simulated plus observed concentrations in the vertical profile boreholes in 2003, respectively. The observed Sr-90 concentrations from 2001 sampling is illustrated in Figure B-38.

The current Sr-90 contamination in the aquifer near INTEC is most likely derived primarily from the injection well. The bulk of the Tank Farm and soil contamination Sr-90 has not yet reached the aquifer because of retardation in the vadose zone. The injection well Sr-90 will remain near INTEC longer than the other simulated contaminants because of retardation in the aquifer. Aquifer concentrations should decrease in the near hture, but would begin to increase if surface recharge cannot be reduced during the OU 3-13, Group 4 remedial actions. As with the Tc-99 simulations, the current model Sr-90 from the vadose zone appears to be spread over a larger area than the 2001 groundwater sampling indicates.

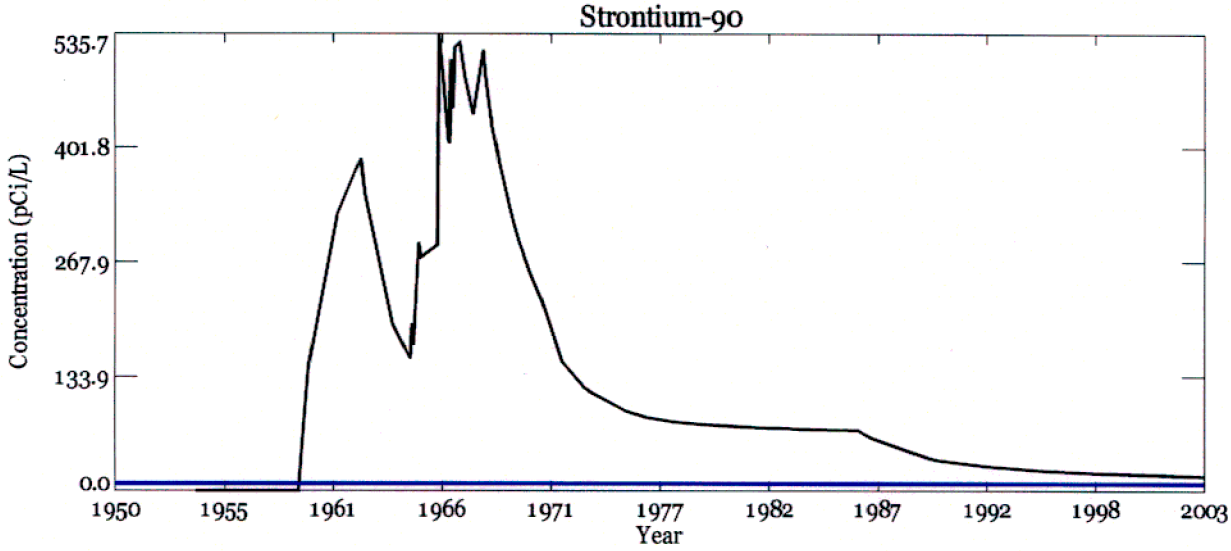

Figure B-34. Simulated Sr-90 peak aquifer concentrations (the blue line is the MCL).

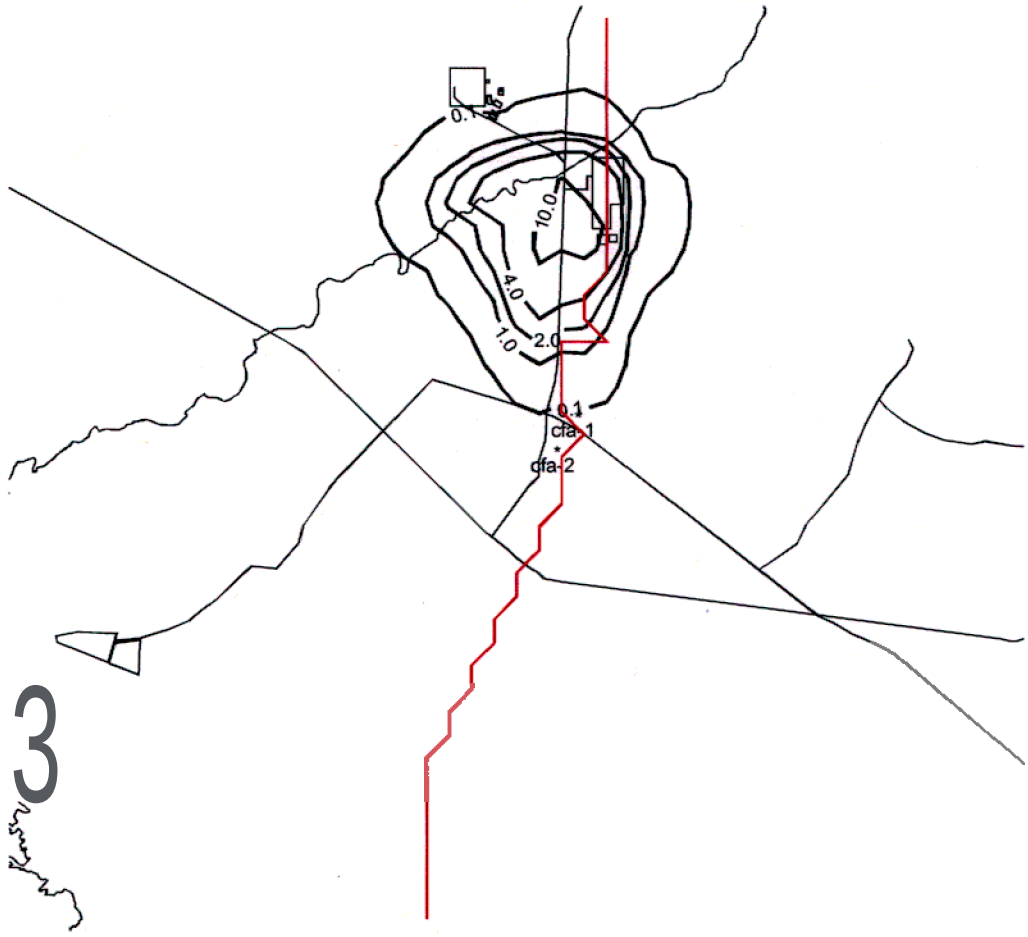

Figure B-35. Simulated Sr-90 concentrations (pCi/L) at the water table in 2001 (the thick red line is a fence diagram cross-section for Figure B-36).

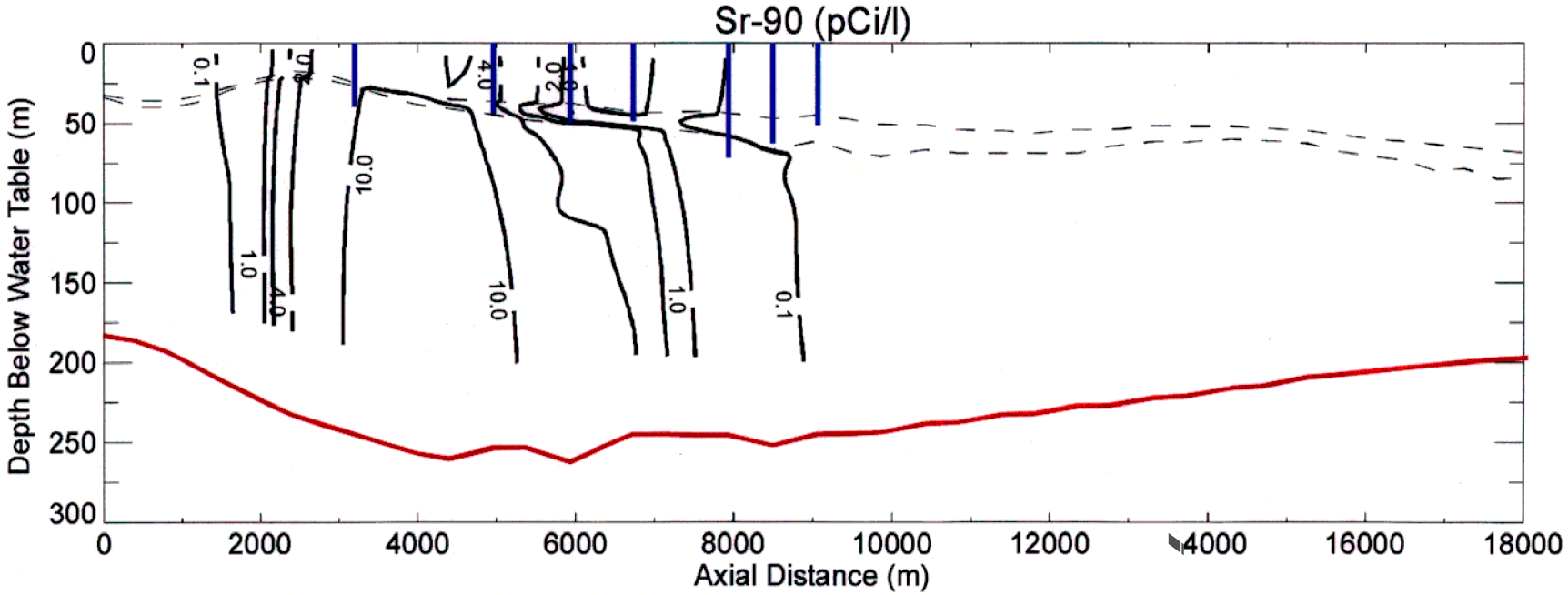

Figure B-36. Simulated Sr-90 vertical concentrations in 2003 (the blue lines are well locations and red line is aquifer bottom).

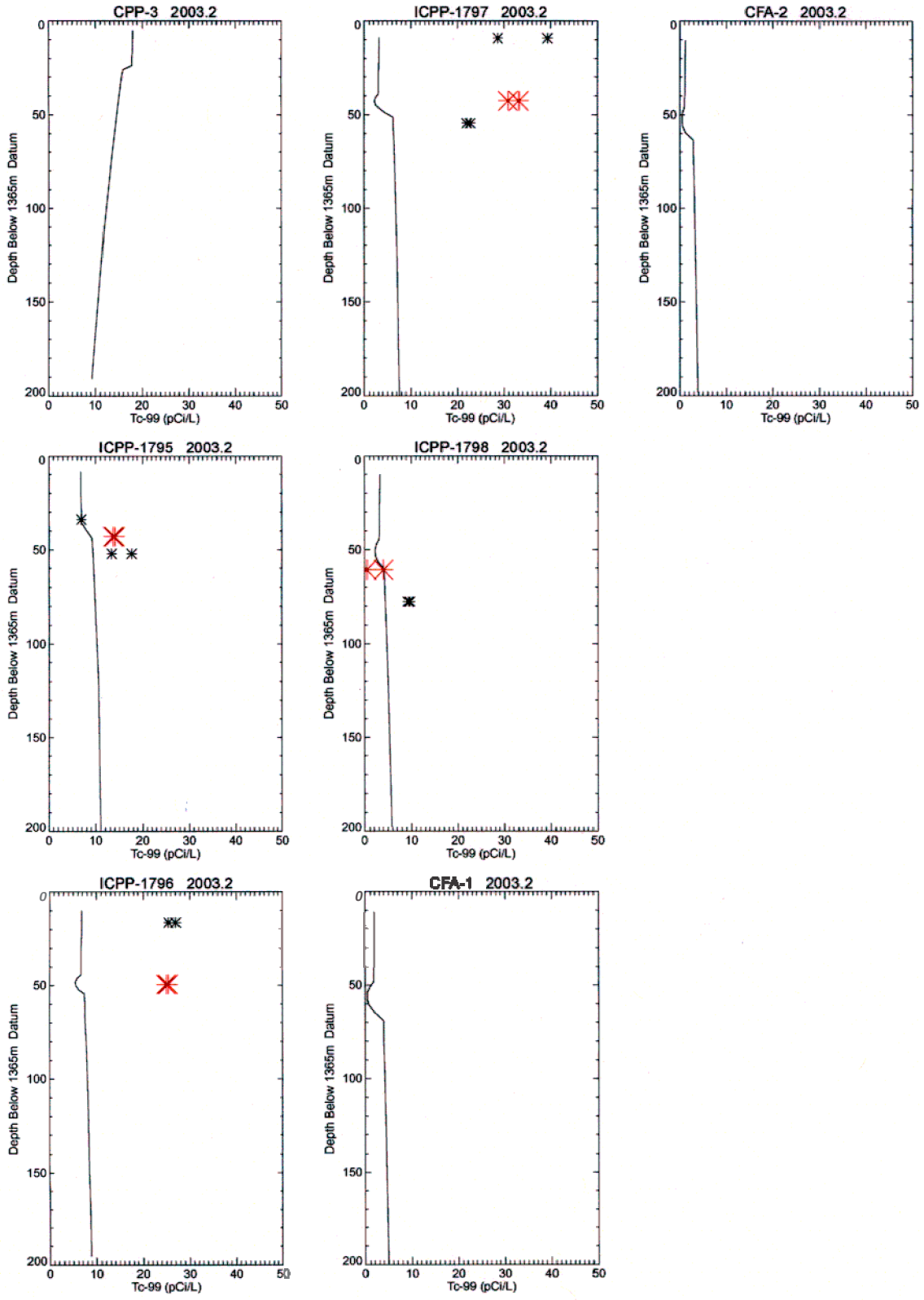

Figure B-37. Simulated Sr-90 versus measured concentrations at vertical boreholes in 2003 (the solid line is simulated, the small asterisk is measured basalt, and the large asterisk is measured HI interbed).

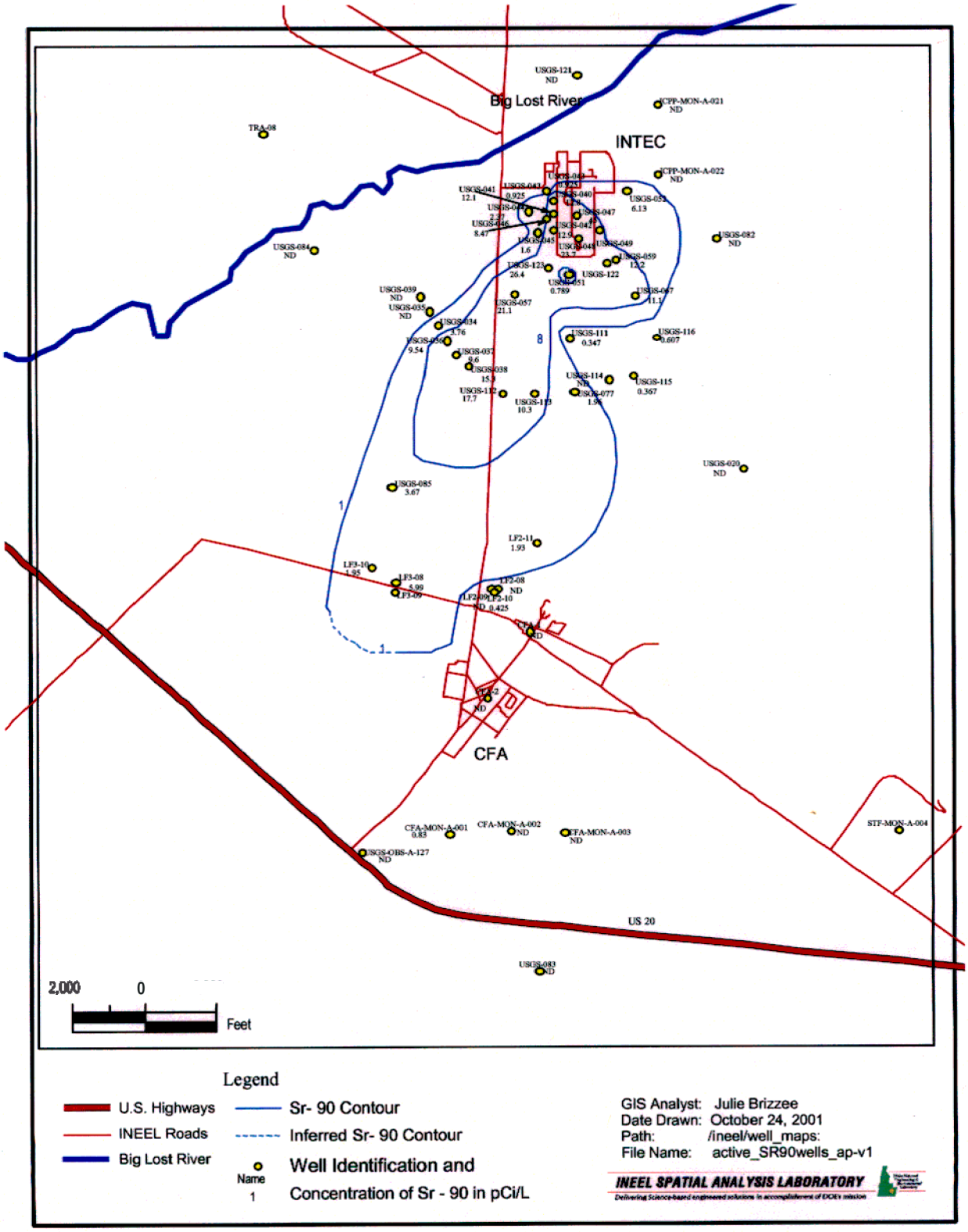

Figure B-38. Observed Sr-90 aquifer concentrations in 2001.

B-4. CONCLUSIONS

The current I-129, tritium, and Tc-99 concentrations in the aquifer near INTEC are most likely the result of vadose zone contaminant sources because these contaminants are very mobile, the injection well ceased regular operation in 1984, and the aquifer velocity is approximately 2 m/day. The current Sr-90 concentrations remaining in the aquifer are most likely the result of Sr-90 disposed of in the former injection well, because Sr-90 movement is retarded and the vadose zone surface sources should not have reached the aquifer by this time. These conclusions are based on the conceptual and numerical modeling assumptions presented in this document.

The current discrepancies between the latest aquifer contaminant observations near INTEC and the model are partially due to poor understanding of the vadose zone water and contaminant travel times. Thus, as the OU 3-14 vadose zone model development provides better understanding of INTEC vadose zone processes, the WAG 3 aquifer model will be updated again in the OU 3-14 model development work.

Matching the observed tritium concentrations in the vertical profile boreholes (ICPP-1795, ICPP-1796, ICPP-1797, and ICPP-1798) required increasing the RI/BRA model flux rate by a factor of 2.5. This suggests contaminant movement through the vadose zone is occurring faster than the RI/BRA predicted or additional tritium sources are present in the vadose zone that were not considered in the RI/BRA modeling.

The RI/BRA model's vadose zone contamination footprint is larger than that observed. This results in the current model over-estimating the aquifer contamination resulting from vadose zone sources in directions lateral and upgradient to the aquifer flow direction and under-estimating peak aquifer concentrations directly beneath and downgradient of INTEC.

The I-129 contamination in the HI interbed most likely does not represent the continuing risk as the RI/BRA modeling predicted because the RI/BRA I-129 source may have been over-estimated and the HI interbed permeability may have been under-estimated. The current model and revised I-129 source term still over-predicts I-129 concentrations in the vertical profile boreholes, but to a lesser degree.

B-5. REFERENCES

Anderson, S. R. and B. D. Lewis, 1991, *Stratigraphy of the Unsaturated Zone at the Radioactive Waste Management Complex, Idaho National Engineering Laboratory, Idaho,* USGS Water-Resource Report 89-4065 (IDO-22080).

DOE-ID, 1989, *Stratigraphy of the Unsaturated Zone at the Radioactive Waste Management Complex, Idaho National Engineering Laboratory, Idaho,* U.S. Geological Survey Water-Resources Investigations Report 89-4065, Idaho Falls, Idaho.

DOE-ID, 1991, *Stratigraphy of the Unsaturated Zone and Uppermost Part of the Snake River Plain Aquifer at the Idaho Chemical Processing Plant and Test Reactor Area, Idaho National Engineering Laboratory, Idaho,* U.S. Geological Survey Water-Resources Investigations Report 91-4010, Idaho Falls, Idaho.

DOE-ID, 1997, *Comprehensive RI/FS for the Idaho Chemical Processing Plant OU 3-13 at the INEEL Part A, RI/BRA Report (Final),* DOE/ID-10534, Rev. *0,* U.S. Department of Energy Idaho Operations Office, November 1997.

DOE-ID, 2000, *Remedial Design/Remedial Action Scope of Work for Waste Area Group 3, Operable Unit 3-13,* DOE/ID-10721, Rev. 1, U.S. Department of Energy Idaho Operations Office, February 2000.

DOE-ID, 2002, *Plume Evaluation Field Sampling Plan for Operable Unit 3-13, Group 5, Snake River Plain Aquifer,* DOE/ID-10784, Rev. 2, U.S. Department of Energy Idaho Operations Office, July 2002.

DOE-ID, 2003, *Phase I Monitoring Well and Tracer Study Report for Operable Unit 3-13, Group 4, Perched Water,* DOE/ID-10967, Rev. 1, U.S. Department of Energy Idaho Operations Office, June 2003. (Note: Rev. 1 is approved for public release; Rev. 2 approval is Official Use Only.)

EDF-3213, 2003, "Idaho Nuclear Technology and Engineering Center Large-Scale Tracer Test Numerical Simulation (Draft)," Idaho Completion Project, December 2003.

Frederick, D. B and G. S. Johnson, 1996, "Estimation of Hydraulic Properties and Development of a Layered Conceptual Model for the Snake River Plain Aquifer at the Idaho National Engineering Laboratory, Idaho," State of Idaho INEL Oversite Program, Idaho Water Resources Research Institute, February 1996.

Magnuson, S. O., 1995, *Inverse Modeling for Field-Scale Hydrologic and Transport Parameters of Fractured Basalt,* INEL-95/0637, Rev. *0,* Idaho National Engineering Laboratory, December 1995.

McCarthy, J.M., R. C. Arnett, R. M. Neupauer, M. J. Rohe, and C. Smith, 1995, *Development of a Regional Groundwater Flow Model for the Area of the Idaho National Engineering Laboratory, Eastern Snake River Plain Aquifer,* INEL-95/0169 (formerly EGG-ER-11490), Rev. 1, Idaho National Engineering Laboratory, March 1995.

Smith, R. P., 2002, *Aquifer Thickness Assessment for Use in WAG 10, OU 10-08 Groundwater Modeling Activities,* INEEL/INT-01-01458 Rev. 0, Idaho National Engineering and Environmental Laboratory, February 2002.

Vinsome, P. K. W. and G. M. Shook, 1993, "Multi-Purpose Simulation," *Journal of Petroleum Science and Engineering*, Vol. 9, pp. 29–38, Elsevier Science Publishers, B. V., Amsterdam.